



NAVAL POSTGRADUATE SCHOOL

MONTEREY, CALIFORNIA

THESIS

**ASSESSING THE FLIGHT QUALITY OF A LARGE
UAV FOR SENSORS/GROUND ROBOTS AERIAL
DELIVERY**

by

Andreas Archontakis

September 2010

Thesis Co-Advisors:

O. Yakimenko

A. Bordetsky

Second Reader:

P. Ateshian

Approved for public release; distribution unlimited

THIS PAGE INTENTIONALLY LEFT BLANK

REPORT DOCUMENTATION PAGE			<i>Form Approved OMB No. 0704-0188</i>	
Public reporting burden for this collection of information is estimated to average 1 hour per response, including the time for reviewing instruction, searching existing data sources, gathering and maintaining the data needed, and completing and reviewing the collection of information. Send comments regarding this burden estimate or any other aspect of this collection of information, including suggestions for reducing this burden, to Washington headquarters Services, Directorate for Information Operations and Reports, 1215 Jefferson Davis Highway, Suite 1204, Arlington, VA 22202-4302, and to the Office of Management and Budget, Paperwork Reduction Project (0704-0188) Washington DC 20503.				
1. AGENCY USE ONLY (Leave blank)		2. REPORT DATE September 2010	3. REPORT TYPE AND DATES COVERED Master's Thesis	
4. TITLE AND SUBTITLE: Assessing the Flight Quality of a Large UAV for Sensors/Ground Robots Aerial Delivery			5. FUNDING NUMBERS	
6. AUTHOR(S) Andreas Archontakis				
7. PERFORMING ORGANIZATION NAME(S) AND ADDRESS(ES) Naval Postgraduate School Monterey, CA 93943-5000			8. PERFORMING ORGANIZATION REPORT NUMBER	
9. SPONSORING / MONITORING AGENCY NAME(S) AND ADDRESS(ES) N/A			10. SPONSORING / MONITORING AGENCY REPORT NUMBER	
11. SUPPLEMENTARY NOTES The views expressed in this Thesis are those of the author and do not reflect the official policy or position of the Department of Defense or the U.S. Government.				
12a. DISTRIBUTION / AVAILABILITY STATEMENT Approved for public release; distribution is unlimited.			12b. DISTRIBUTION CODE A	
13. ABSTRACT (maximum 200 words) The new goal for unmanned aerial systems will be to find creative methods of keeping the cost low and still maintain effectiveness. This thesis discusses the importance of UAVs over the last few years, suggests the development of a low-cost, large UAV, and evaluates the results. We also examine the idea of a platform for deploying multiple aerial-delivery, parafoil-based systems and discuss scenarios for the improvement of the collaboration of the large UAV with the Snowflake project.				
14. SUBJECT TERMS UAV, Network, LinAir software, Simulink, GSM, TNT, VoT, Snowflake, TNT tesbed, MANET.			15. NUMBER OF PAGES 71	
			16. PRICE CODE	
17. SECURITY CLASSIFICATION OF REPORT Unclassified	18. SECURITY CLASSIFICATION OF THIS PAGE Unclassified	19. SECURITY CLASSIFICATION OF ABSTRACT Unclassified	20. LIMITATION OF ABSTRACT UU	

NSN 7540-01-280-5500

Standard Form 298 (Rev. 2-89)
Prescribed by ANSI Std. Z39-18

THIS PAGE INTENTIONALLY LEFT BLANK

Approved for public release; distribution is unlimited

**ASSESSING THE FLIGHT QUALITY OF A LARGE UAV FOR
SENSORS/GROUND ROBOTS AERIAL DELIVERY**

Andreas Archontakis
Major, Hellenic Airforce
BS, Hellenic Airforce Academy, 1995

Submitted in partial fulfillment of the
requirements for the degree of

MASTER OF SCIENCE IN INFORMATION WARFARE

from the

NAVAL POSTGRADUATE SCHOOL

Author: Andreas Archontakis

Approved by: Oleg Yakimenko
Thesis Advisor

A. Bordetsky
Co-Advisor

P. Ateshian
Second Reader

Dan C. Boger, PhD
Chairman, Department of Information Sciences

THIS PAGE INTENTIONALLY LEFT BLANK

ABSTRACT

The new goal for unmanned aerial systems will be to find creative methods of keeping the cost low and still maintain effectiveness. This thesis discusses the importance of UAVs over the last few years, suggests the development of a low-cost, large UAV, and evaluates the results. We also examine the idea of a platform for deploying multiple aerial-delivery, parafoil-based systems and discuss scenarios for the improvement of the collaboration of the large UAV with the Snowflake project.

THIS PAGE INTENTIONALLY LEFT BLANK

TABLE OF CONTENTS

I.	INTRODUCTION.....	1
A.	PROBLEM	1
B.	OBJECTIVES	1
C.	THESIS STRUCTURE	2
II.	UNMANNED SYSTEMS	3
A.	UAVS.....	3
B.	THE MQ-9 REAPER	4
III.	DERIVATIVE COEFFICIENTS OF PITBULL UAV	7
A.	BASIC IDEA	7
B.	LINAIR MODELING	11
C.	MODELING.....	26
IV.	NETWORKING THE UAV.....	31
A.	GSM NETWORK.....	31
B.	VOICE ON TARGET	33
C.	TNT TESTBED.....	35
V.	PITBULL-SNOWFLAKE COLLABORATION.....	37
A.	SNOWFLAKE.....	37
B.	PITBULL AS A CARRIER OF SNOWFLAKES.....	39
C.	MULTIPLE SNOWFLAKES CREATING AN AD-HOC NETWORK ..	42
VI.	CONCLUSIONS	47
	LIST OF REFERENCES	49
	INITIAL DISTRIBUTION LIST	51

THIS PAGE INTENTIONALLY LEFT BLANK

LIST OF FIGURES

Figure 1.	The MQ-9 Reaper	5
Figure 2.	Side view of a prototype carrier.....	7
Figure 3.	Top view of a prototype carrier	8
Figure 4.	Front view of a prototype carrier	9
Figure 5.	Main wing (a) and horizontal/vertical stabilizer airfoils.....	9
Figure 6.	Side, top, and front view of the LinAir Pro panel model.....	12
Figure 7.	Lift force distribution at $\alpha = 3^\circ$ (upper left), $\alpha = 10^\circ$ (upper right)) and $\alpha = -5^\circ$ (down)	13
Figure 8.	Results of the α -sweep at $\beta = 0^\circ$ (left) and β -sweep at $\alpha = 3^\circ$ (right)	14
Figure 9.	Results of the α -sweep at $\beta = -10^\circ$ (left) and $\beta = 10^\circ$ (right).....	14
Figure 10.	Results of the β -sweep at $\alpha = -5^\circ$ (left) and $\alpha = 10^\circ$ (right)	14
Figure 11.	Results of the α -sweep at $\hat{q} = 1$	15
Figure 12.	Results of the β -sweep at $\hat{p} = 1$ (left) and $\hat{r} = 1$ (right).....	15
Figure 13.	Geometry (left) and effect (right) of a 15° aileron deflection.....	16
Figure 14.	Geometry (left) and effect (right) of a 10° elevator deflection.....	16
Figure 15.	Figure 15: Geometry (left) and effect (right) of a 10° rudder deflection.....	16
Figure 16.	Geometry (left) and effect (right) of a 10° flaps deflection	17
Figure 17.	Simulink model for finding trip conditions	26
Figure 18.	Pitbull longitudinal channel at trim condition	27
Figure 19.	Pitbull lateral channel at trim condition.....	27
Figure 20.	Pitbull longitudinal channel with 10N throttle increase	28
Figure 21.	Pitbull longitudinal channel with 1 degree elevator deflection	29
Figure 22.	Pitbull lateral channel with 1 degree aileron deflection.....	29
Figure 23.	Pitbull lateral channel with 1 degree rudder deflection	30
Figure 24.	Existing GSM Network Coverage	31
Figure 25.	The structure of a GSM network	32
Figure 26.	Voice-on-Target Portal Infrastructure.....	34
Figure 27.	Plug-and-Play testbed with global reachback [7]	36
Figure 28.	Snowflake with parafoil (a) and avionics (b).....	38
Figure 29.	The Snowflake communication architecture [8].....	40
Figure 30.	UAVs creating ad-hoc network	43
Figure 31.	Group of UAVs carrying Snowflakes developing a short-term aerial ad-hoc network.....	45
Figure 32.	Multiple Mobile Ad-hoc NETWORKS (MANETs) controlled by multi-users...	46

THIS PAGE INTENTIONALLY LEFT BLANK

LIST OF TABLES

Table 1.	Aerodynamic and control derivatives for different aircraft	19
Table 2.	Geometry and mass/inertia data for different aircraft	21

THIS PAGE INTENTIONALLY LEFT BLANK

LIST OF ACRONYMS AND ABBREVIATIONS

ADS	Aerial Delivery System
AOA	Angle Of Attack
BSS	Base Station Subsystem
BDA	Battle Damage Assessment
CEP	Circular Error Probable
DOE	Department of Energy
DHS	Department Homeland Security
EDGE	Enhanced Data for GSM Environment
ENU	East North Up
EGBU	Electro-optical Guidance Bomb Unit
GBU	Guidance Bomb Unit
GNC	Guidance Navigation Control
GPRS	General Packet Radio Service
GPS	Global Positioning System
GSM	Global System of Mobile
HLD	Homeland Defense
ISR	Intelligence, Surveillance, and Reconnaissance
JDAM	Joint Direct Attack Munition
MANET	Moving Ad-hoc Network
MOI	Moment Of Inertia
MTS	Multi-Spectral Targeting System
NASA	National Aeronautics and Space Administration
NOC	Network Operations Center
NSS	Network Subsystem
OSD	Office of Secretary of Defense
SEAD	Suppression of Enemy Air Defenses
SMS	Short Message Service
TNT	Tactical Network Topology
UAV	Unmanned Aerial Vehicle
VOT	Voice On Target

THIS PAGE INTENTIONALLY LEFT BLANK

EXECUTIVE SUMMARY

The new goal for unmanned aerial systems will be to find creative methods of keeping the cost low and still maintain effectiveness. This thesis discusses the importance of UAVs over the last few years, suggests the development of a low-cost, large UAV, and evaluates the results. We also examine the idea of a platform for deploying multiple aerial-delivery, parafoil-based systems and discuss scenarios for the improvement of the collaboration of the large UAV with the Snowflake project.

THIS PAGE INTENTIONALLY LEFT BLANK

ACKNOWLEDGMENTS

I would like to thank Professor Yakimenko for his valuable help and guidance, and all the other professors and teachers who made my journey into knowledge a long and worthwhile experience.

THIS PAGE INTENTIONALLY LEFT BLANK

I. INTRODUCTION

A. PROBLEM

The increasing demand for information in warfare, especially in conflict zones such as Afghanistan and Iraq, have created the need for developing platforms, networks, and other systems to improve the Intelligence, Surveillance, and Reconnaissance (ISR) capability, situation awareness and effectiveness in the battlefield.

B. OBJECTIVES

Modeling and simulation are the tools that allow verification and further evaluation of our designs with safety, less cost and the risk of flying an unmanned aircraft (UAV). Changes and modifications are much easier after new inputs and test results.

LinAir is a very reliable and simple program that computes aerodynamic properties based on the dimensions of the model's parts. The program can generate the effect of different angles of attack, side slip angles with parallel deflections of the control surfaces and turn rate inputs. Companies such as Northrop, Lockheed, Boeing and NASA have used LinAir because of its simplicity, as well as its reliability for generating quick results.

The results of the procedures with the LinAir program are the aerodynamic and control derivatives that will be used for evaluation at the Simulink Model. This model allows us to find trimming conditions, system dynamics simulation, and system identification computing aerodynamic forces and moments.

Furthermore, the collaboration between UAVs and networking for controlling the missions, receiving and sending data from a cell phone by voice or through the Internet is a capability that can add flexibility to missions and better control of unmanned platforms from a distance.

The cooperation of the UAV-Snowflake system with the TNT testbed through GSM and Internet can be an alternative approach for communication between man and the tactical network environment.

C. THESIS STRUCTURE

In Chapter II, we discuss some existing platforms and their use in Information Warfare. In Chapter III, we calculate the aerodynamic coefficients for the large UAV model.

In Chapter IV, we review the GSM network, VoT and TNT testbed. In Chapter V, we discuss and analyze some tactical scenarios using large UAVs carrying parafoil systems (like Snowflake) and controlled by GSM and TNT testbed networks. In Chapter VI, we discuss some conclusions and future work.

II. UNMANNED SYSTEMS

A. UAVs

A very basic conclusion that arises from recent wars is that public opinion and the media are against loss of life during a war, and even more so during peace operations such as in Kosovo. Governments have to deal with the pressure from these situations because the political cost is high. For this reason, in recent decades, many countries have developed a large variety of Unmanned Air Vehicles (UAVs), and they are now part of any modern army.

The first UAV missions are dated from roughly a half century ago in the U.S. Specifically, in 1959, the Ryan Aeronautical Company conducted a study to investigate how the UAV Firebee could be used for missions' strategic recognition of big beams. "Firebee" was a small objective that presented low prices for reflective surfaces, rendering its localization from the radars of that era. These flights, over the USSR, and their collection of strategic information were considered a gamble. The engineers of the company believed that they could increase the endurance of the vehicle to the point where, after its launch from the Barents Sea north of the Soviet Union, it would be able to fly south across the entire country and be recovered in Turkey.

The 100th Wing of Strategic Recognition was created in 1964, and included, exclusively, the "Lightning Bugs" located on the island of Okinawa. The wing was used successfully on these vehicles in missions of recognition over Vietnam, Korea and China in the 1960s and 1970s, and it has performed over 3,000 exits.

The development of this technology provided the advantage of using it in a large range of roles during subsequent wars. Their primary mission, as it was in the first steps of the operations, remained the collection and transmission of information in real time for surveillance, recognition and targeting, which are today's ISTAR (Intelligence Surveillance Target Acquisition Reconnaissance) missions.

Moreover, in the ISTAR missions, UAVs are used for SEAD (Suppression Enemy Air Defense) and BDA (Battle Damage Assessment) missions. Finally, other than military applications, UAVs are also used in police and government services.

There are many reasons, in our era, why unmanned systems are more and more attractive and feasible. Technology, including weapons, payloads, and sensors, are smaller and more capable of providing better ratios between capabilities and weight. New materials and advanced microprocessors, software, global positioning systems, and modern autopilots provide higher accuracy in navigation and delivery system development.

Unmanned systems have the advantage of operating in environments that are non-allowable for manned systems, such as biological, radioactive or chemical, and they are capable of getting close to the targets and sending the information directly to the center of the operation.

B. THE MQ-9 REAPER

For over sixty years, the U.S. military has employed a large number of UAV systems. In the recent history of UAVs, the U.S. started to purchase Israeli unmanned systems and began developing the new generation of UAVs such as the Predator A-RQ1. From 1996 until 2004, Predator was included in most major missions and logged over 100,000 hours, about 70 percent of which were in the operational environment. Another version of Predator, the MQ-1, is one of the most famous and requested systems for missions in the war on terrorism.

In the past two years, the USAF has increased the total number of UAVs by 300 percent. This shows the importance of these kinds of systems, and in parallel, the USAF plans to shift over 3,500 manpower billets for collecting and analyzing data from UAVs.



Figure 1. The MQ-9 Reaper

A recent example of a successful UAV is the MQ-9 Reaper (originally called Predator B) a long distance, medium-high altitude UAV used for surveillance and reconnaissance missions. Its missions use a synthetic aperture, radar, cameras, and infrared sensors and it has the capability of a real-time communication link between the battlefield and the commander. The Raytheon multi-spectral targeting system (MTS-S), which can be carried from an MQ-9, can provide laser designation capabilities as well as TV/infrared real-time pictures. Also, the synthetic aperture radar has a resolution of one foot and provides all-weather surveillance capabilities. The entire mission can be controlled through line-of-sight data links or by satellite via Ku band and produce real-time video. The operator can “send” a command, and it takes about 1.2 seconds to reach the drone from the satellite link.

Predators (Reaper MQ-9 is the Air Force version) have flown over 500,000 hours in Afghanistan and Iraq, but at the same time, the Federal Aviation Administration certified Reapers to fly over the U.S. for search-and-rescue purposes during Hurricane Katrina—and with great results.

The Predators' operational ceiling is about 50,000 feet. They can carry Hellfire II missiles, laser bomb GBU-12s (or the electroptical version EGBU-12), a GBU-38 JDAM (joint direct attack munition) and a GBU-49 Enhanced Paveway II [1].

Instead of munitions, they can carry cameras coupled with infrared sensors that can zoom in on pirates from 50,000 feet when patrolling over the waters of Somalia. Reapers help international authorities by recording the movements of suspected pirates. This is very important because, as the crimes unfold in this area, it is too difficult for the authorities to respond in time to catch the pirates. Even when they can, the pirates have plenty of time to hide their weapons and booty. So, for lack of evidence, the authorities have to release them. By recording these activities, the authorities can build a case and solve this problem.

III. DERIVATIVE COEFFICIENTS OF PITBULL UAV

A. BASIC IDEA

The UAV model on which we calculate the derivative coefficients is based on the geometry and design of a prototype aircraft called the Pitbull X-2. The goal is that by calculating the derivative coefficients for the Pitbull X-2, we can use the results for our large UAV and evaluate them with Simulink.

Geometry of the deployment platform prototype:

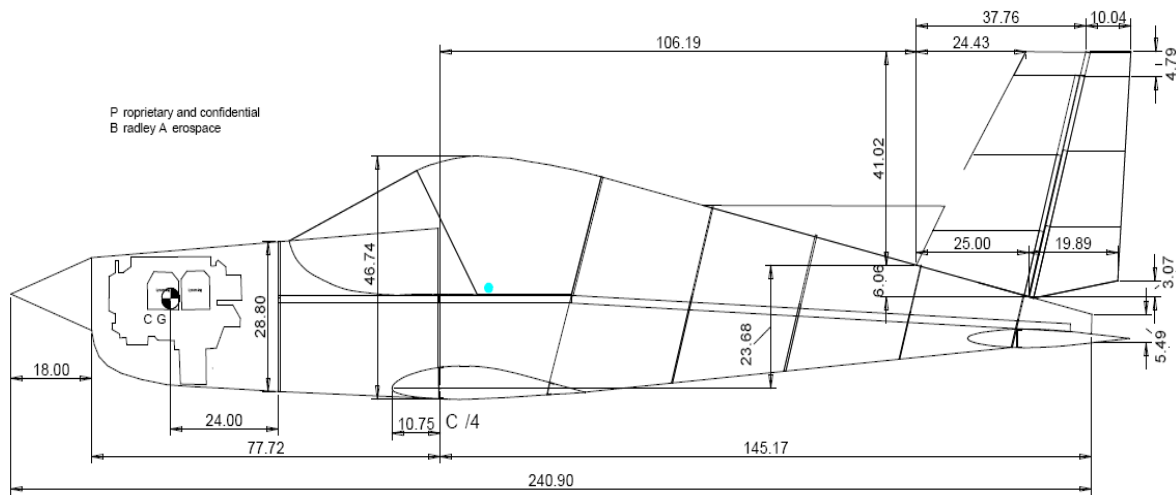


Figure 2. Side view of a prototype carrier

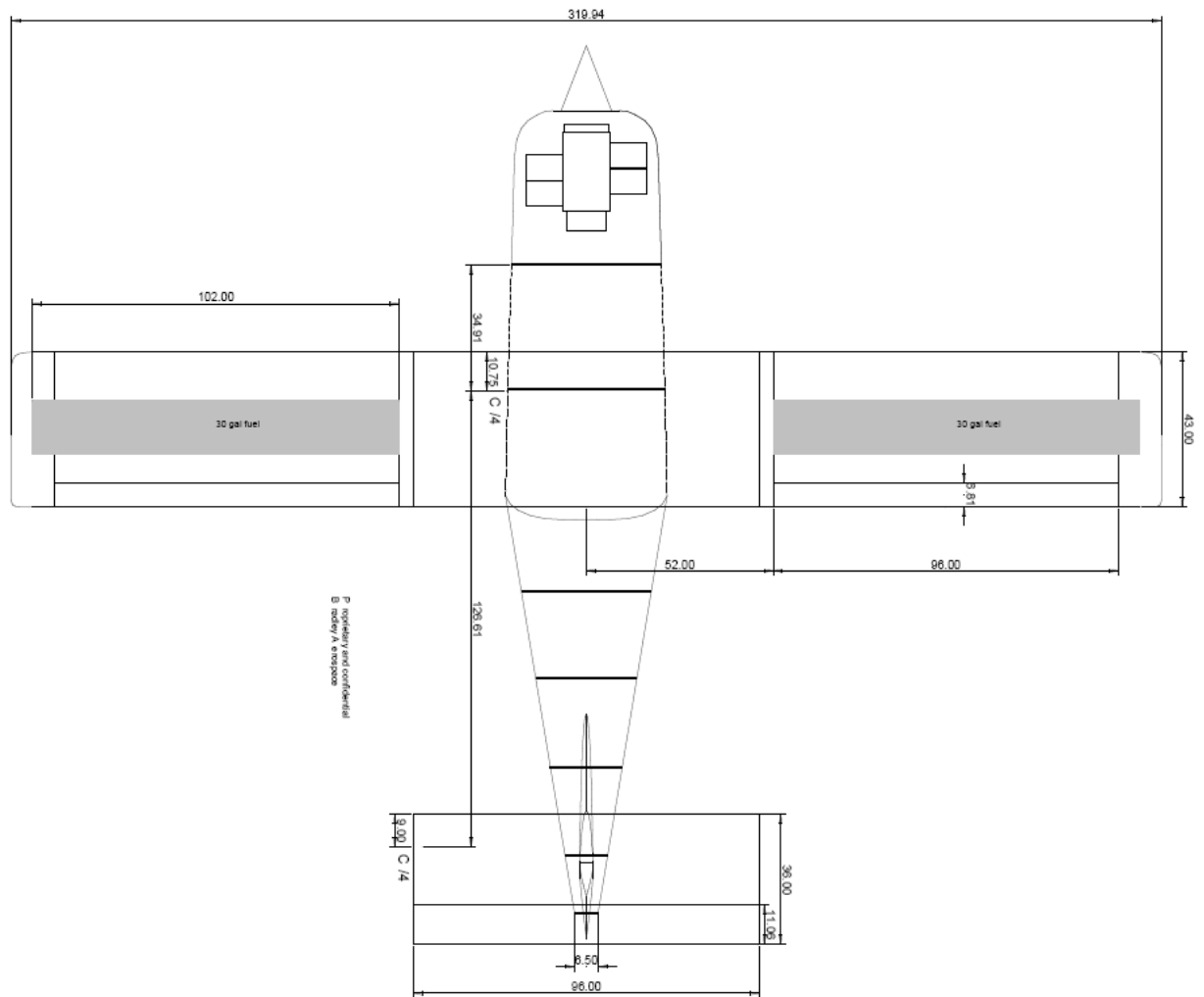


Figure 3. Top view of a prototype carrier

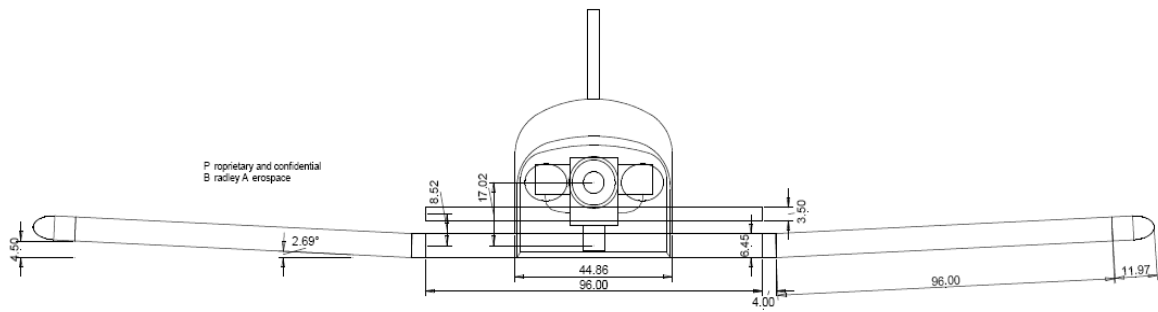


Figure 4. Front view of a prototype carrier

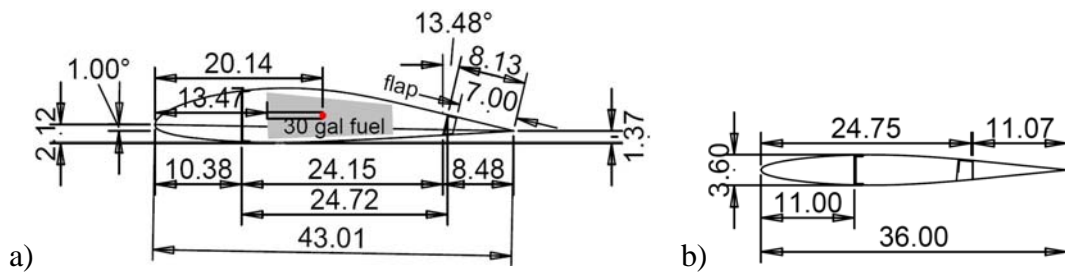


Figure 5. Main wing (a) and horizontal/vertical stabilizer airfoils

The prototype Pitbull X-2 has the following characteristics

1. Empty weight — 850 Pounds
2. Gross Weight — 1730 pounds speed wing
3. Power loading — $7.5 = 200\text{hp}$ - $10 = 150\text{hp}$ - $15 = 100\text{hp}$ $14.2 = 100\text{hp}$

L.S.A.

4. Wing loading — 15.30 on speed wing. 11.26 on L.S.A.
5. Useful load — 880 pounds
6. Fuel in Gallons — 58 gallons
7. Engines used — Lycoming 0320 - 0360 - Continental 0200 or any 100-200hp
8. Wheels/Brakes — Matco only
9. Wing skins — 2024-T3 alclad aircraft grade only (No 6061-T6 skins used)
10. Fuel tanks — Aluminum fuel tanks in each wing
11. Wing tips — Wing tips have flush fuel caps and strobes
12. Stick system — Dual stick system
13. Landing gear — Spring steel mains and spring steel nose with castering wheel
14. Canopy — F-15 style rear hinging
15. Fuselage — Semi-monocoque stretched skin and bulkheads
16. Wing — 43"- 35A-415 Riblet corrected (No NACA airfoils)
17. Horz stab — Fully flying tail with full span trim
18. Rivets — Steel/steel and zinc plated pull type rivet
19. Rudder pedals — Dual rudder pedals toe brakes
20. Control systems — Ailerons are 4130 push rods, Rudder #2 push pull housed cables
21. Flaps — Plain top hinged full span worm drive
22. Ailerons — Top hinged full span
23. Bulkheads — 2024-T3 CNC cut.050

- 24. Baggage — 80 pounds behind seats
- 25. Wing area (Speed wing) — 98 sq feet
- 26. Wing area (L.S.A. wing) — 126 sq feet
- 27. G - Loading — Aerobatic to Far-23 9+gs 9-gs
- 28. Spars — A Bradley Aerospace exclusive mil spec extruded spars
- 29. Cabin width — 45 inches wide, Can carry two 250 lb people, 6'8" tall

+ bags

- 30. Take off (Speed wing) — 400 feet
- 31. Landing (Speed wing) — 450 feet
- 32. Take off (LSA) — 325 feet
- 33. Landing (LSA) — 400 feet
- 34. Stall (speed wing no flaps) — 58 mph
- 35. Stall (speed wing/w flaps) — 50 mph
- 36. Stall (LSA) no flaps — 49 mph
- 37. Stall (LSA) /w flaps — 41 mph
- 38. Range — 800 mile range
- 39. Recovery option -B.R.S Onboard recovery system
- 40. Rate of climb — 1800fpm/180hp. 1600fpm/150hp.1320fpm/L.S.A or 100hp

B. LINAIR MODELING

LinAir is a simple and reliable software that helps to compute aerodynamic properties based on the geometry of the model that is created from individual panels. It is capable of generating the effect of varying the angle of attack and sideslip angle, as well as introducing turn rates and deflecting the control surfaces.

After calculating the model dimensions and saving them as a text file, we can upload these files via LinAir and check for visual errors before we start calculating the coefficients.

Our basic model is designed with elements for the following parts:

3 elements for the vertical plane

- 2 elements for the horizontal plane
- 4 elements for each wing
- 2 elements for vertical stabilizer
- 3 elements for the horizontal stabilizer

From the geometry, the reference wingspan is 43 (bref) and the reference area, the projected wings area on the X-Y plane is about 13757.

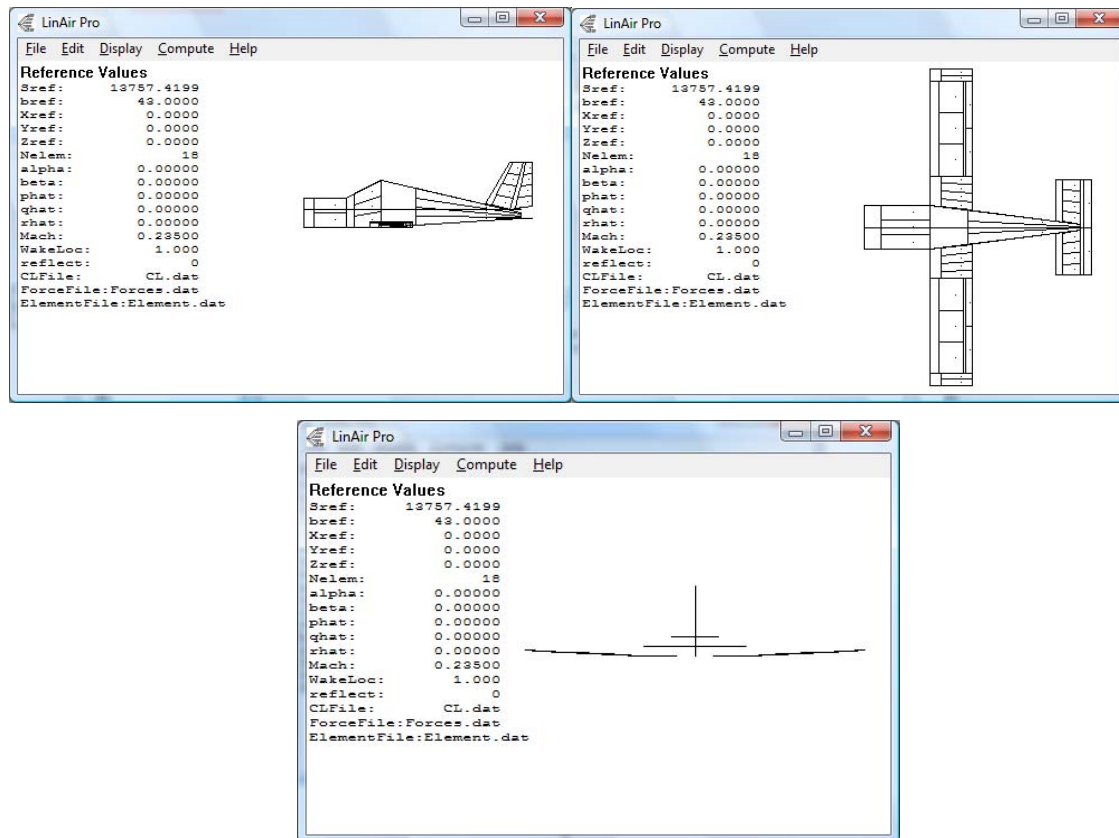


Figure 6. Side, top, and front view of the LinAir Pro panel model

After the model is completed, we perform some tests to see the characteristics of our design. The first test is to verify that the main lift contribution is positive, especially for the wings. The graphs must be symmetrical for all the alpha ranges we applied.

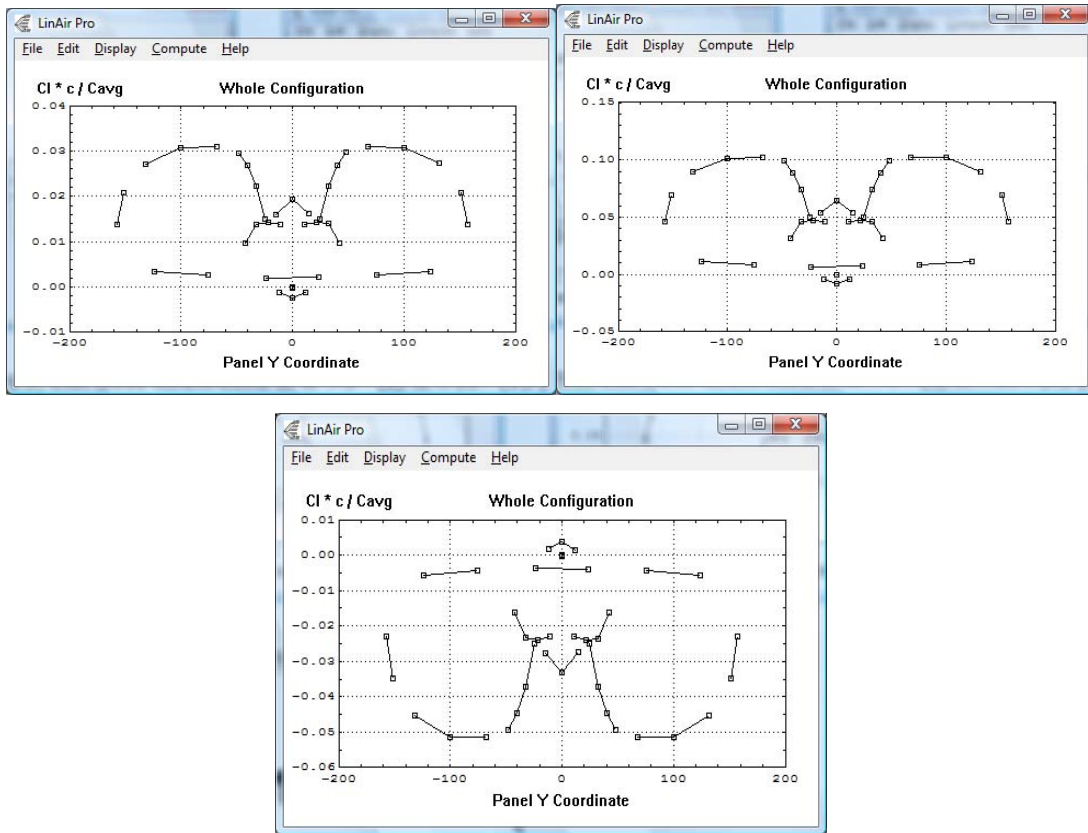


Figure 7. Lift force distribution at $\alpha = 3^\circ$ (upper left), $\alpha = 10^\circ$ (upper right)) and $\alpha = -5^\circ$ (down)

After the first diagnostic checks, runs were performed to find data for the coefficient analysis. The results are based on AOA and vary from -10 to 10 degrees; the beta sweeps from -10 to 10 degrees as well.

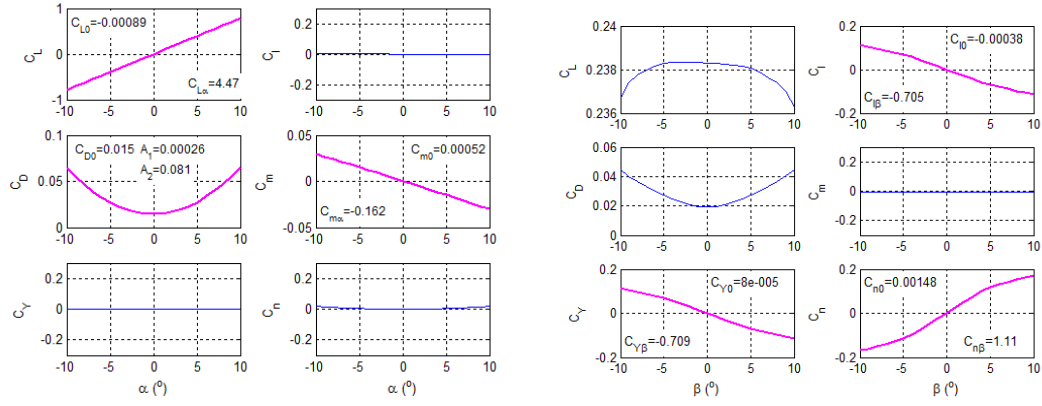


Figure 8. Results of the α -sweep at $\beta = 0^\circ$ (left) and β -sweep at $\alpha = 3^\circ$ (right)

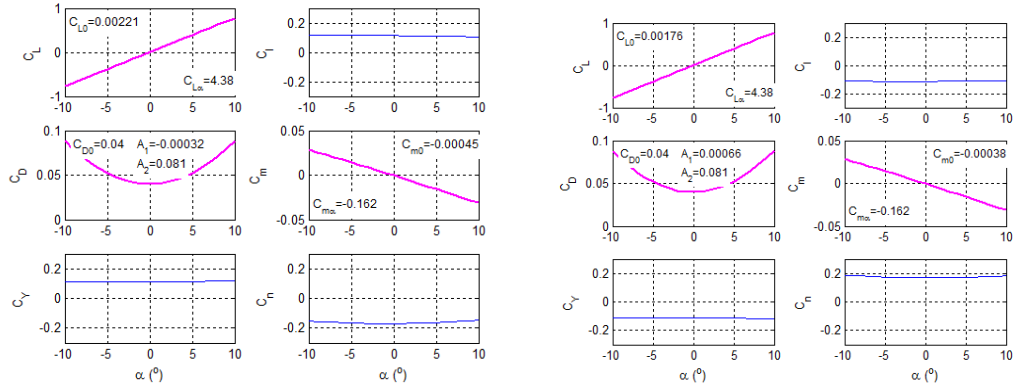


Figure 9. Results of the α -sweep at $\beta = -10^\circ$ (left) and $\beta = 10^\circ$ (right)

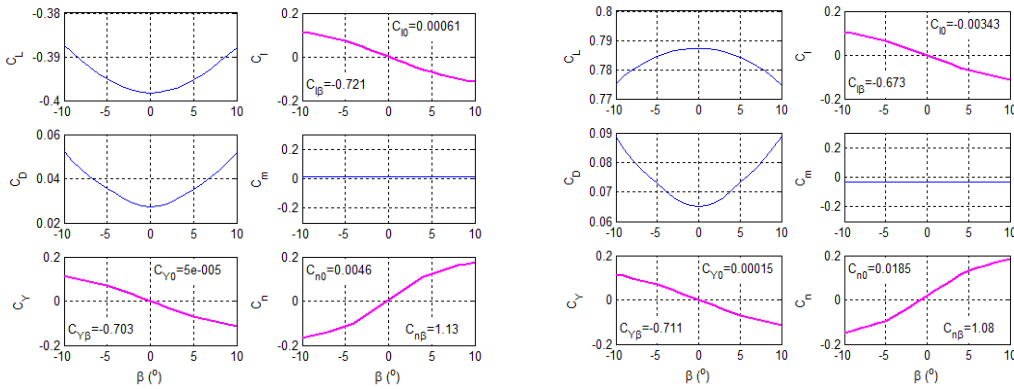


Figure 10. Results of the β -sweep at $\alpha = -5^\circ$ (left) and $\alpha = 10^\circ$ (right)

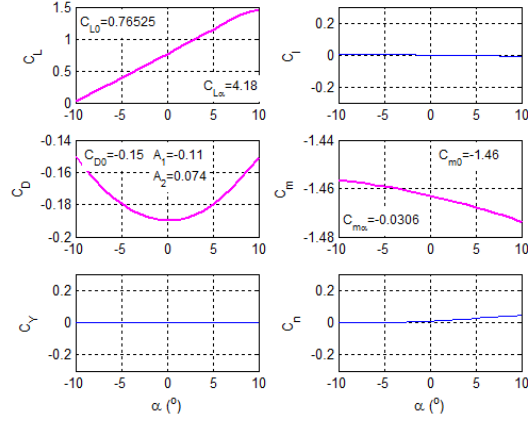


Figure 11. Results of the α -sweep at $\hat{q} = 1$

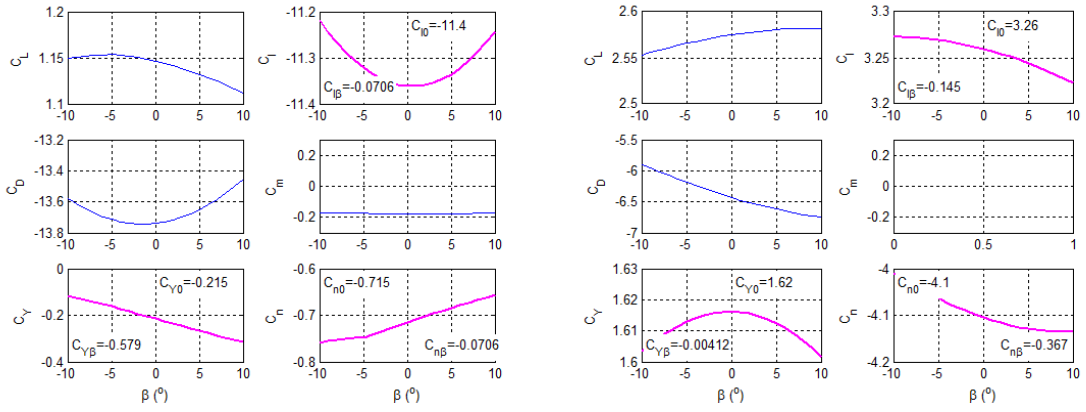


Figure 12. Results of the β -sweep at $\hat{p} = 1$ (left) and $\hat{r} = 1$ (right)

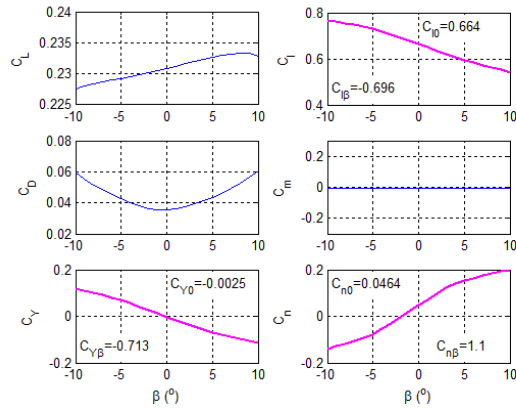
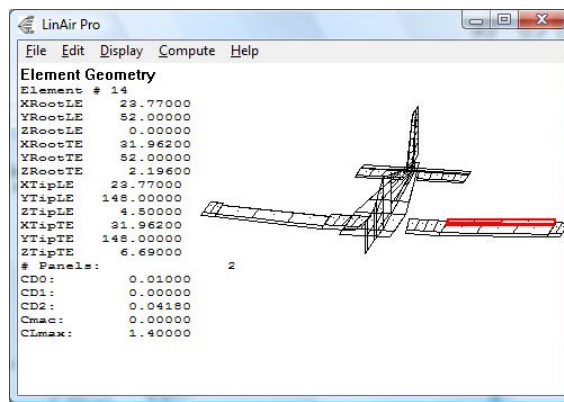


Figure 13. Geometry (left) and effect (right) of a 15° aileron deflection

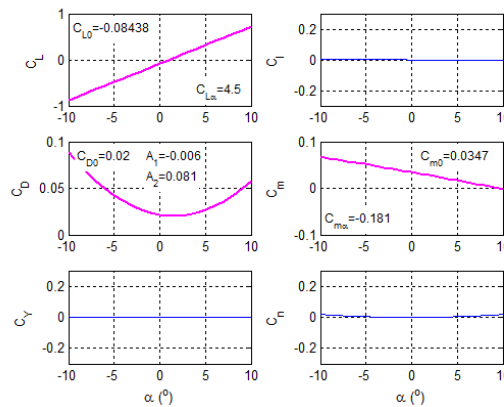
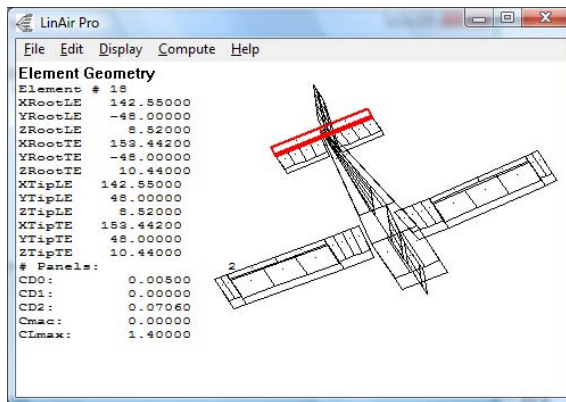


Figure 14. Geometry (left) and effect (right) of a 10° elevator deflection

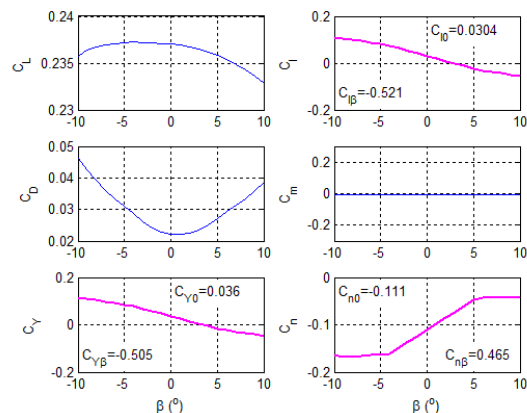
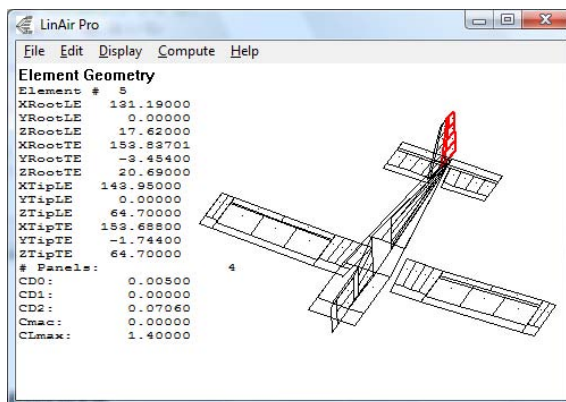


Figure 15. Figure 15: Geometry (left) and effect (right) of a 10° rudder deflection

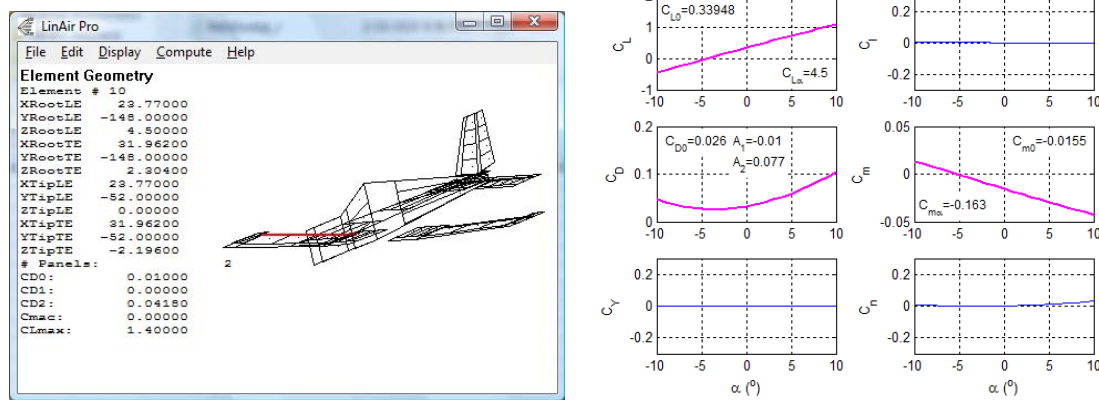


Figure 16. Geometry (left) and effect (right) of a 10° flaps deflection

All these results gave the data to compute the following coefficients:

- Cl_0 is the lift coefficient when the alpha sweep is equal to zero.
- Cl_{α} is the positive gradient of the lift coefficient from CL vs α -sweep curve.
- $Cl_{\alpha \cdot}$ is the average increase of the lift with AOA from -10 to 10 degrees.
- Cl_q is the lift coefficient for the pitch rate of 1 rad/sec without any other deflection.
- $CLDe$ is the lift coefficient due to the elevator deflection. In the Pitbull model, we simulate deflection at -10 and +10 with the same gradient results.
- $CD0$ is the minimum drag coefficient and the value obtained when $CL=0$ from the Cd/Cl curve.
- $A1$ is obtained from the Cd/Cl curve and is the first order lift coefficient.(Figure 11a)
- $A2$ is the second order lift coefficient from the Cd/Cl curve.
- $CDDe$ is the drag coefficient due to the elevator for -10 and +10 degrees of deflection. The gradient was the same for these two values of deflection and the result is based on the deflection per degree.
- Cy_b is the coefficient for the side force due to sideslip, and was obtained from the Cy vs β curve.

- CYDr is the coefficient for the side force, but from the rudder deflection. The deflection values were -10 and +10 degrees and gave the same gradient. So, after calculations, we took the coefficient for the side force per degree of rudder deflection.
- Clb is the coefficient for the dihedral effect.
- Clp is the roll damping. This is the result when applying a 1 rad/sec roll effect at the UAV model without any other control deflections.
- Clr is the resulting roll when a 1 rad/sec yaw rate is applied without any other control deflections.
- CIDa is the roll control power when an aileron deflection is applied. The tested deflections were +15 and -15 degrees, and show that the gradients were the same. Therefore, after calculations, the value obtained is for 1 degree per second applied to get the side roll rate.
- CIDr is the roll caused by a rudder deflection. Rudder deflections tested were 10 and -10 degrees and with the same gradients. Finally, we obtained the value for side roll rate per 1 degree of rudder deflection.
- CM0, which is the pitch moment for AOA, equals zero, and there were no other control deflections.
- CMa is the pitch moment due to AOA. Actually, it is the gradient of the curve CM vs AOA.
- Cma_dot is the pitch moment due to the AOA rate.
- CMq is the pitch moment due to the pitch rate. This value can be obtained by applying 1 rad per second without any control surface.
- CMDe is the pitch control power moment due to the elevator deflection. The deflections were -10 and 10 degrees with the same gradients for CM vs AOA. Finally, the calculated value is the lift due to the deflection of the elevator for 1 degree deflection.
- CNb is the weathercock stability, which indicates an aircraft's ability to return to the previous heading after being yawed by a wind.

- C_{Np} is the adverse yaw coefficient after a 1 rad/sec roll rate without any other deflection.
- C_{Nr} is the yaw damping and was obtained when 1 rad/sec yaw rate was applied.

Table 1. Aerodynamic and control derivatives for different aircraft

		Pioneer	Bluebird	FROG	Old Silver Fox	Old Silver Fox II	New Silver Fox	P10B	P10B AVL	Pitbull
CL0	lift coefficient at $\alpha = 0$	0.385	0.02345	0.4295	0.3260	0.3280	0.3243	0.1719	0.2521	-0.00089
CLα	lift curve slope	4.78	4.1417	4.3034	4.6800	5.0970	6.0204	5.0363	5.0420	4.47
CL$\dot{\alpha}$	lift due to angle of attack rate	2.42	1.5787	1.3877	0.8610	1.9300	1.9300	4.9546	4.8890	2.19
CLq	lift due to pitch rate	8.05	3.9173	3.35	2.5300	6.0300	6.0713	5.6207	5.6436	0.76614
CLδ_e	lift due to elevator	0.401	0.4130	0.3914	0.3510	0.7380	0.9128	0.3690	0.3621	0.4888
CD0	drag coefficient at $C_L = 0$	0.06	0.0311	0.0499	0.0187	0.0191	0.0251	0.0131	0.0129	0.015
A1	drag curve coefficient at C_L	0.43	0.1370	0.23	0.0000	0.0000	-0.0241	0.0002	0.0004	0.00025
A2	drag curve coefficient at C_L^2				0.0413	0.0377	0.0692	0.0777	0.0774	0.081
CDδ_e	drag due to elevator	0.018	0.0650	0.0676	0.0486	0.1040	0.1000	0.0424	0.0431	0.02865
CYβ	side force due to sideslip	-0.819	-0.3100	-0.3100	-0.3100	-0.2040	-0.3928	-0.2865	-0.2922	-0.709
CY\dot{r}	side force due	0.191	0.0697	0.0926	0.0613	0.1120	0.1982	0.1570	0.1587	0.2063

		Pioneer	Bluebird	FROG	Old Silver Fox	Old Silver Fox II	New Silver Fox	P10B	P10B AVL	Pitbull
	<i>to rudder</i>									
Clb	<i>dihedral effect</i>	-0.023	-0.0330	-0.0509	-0.0173	-0.0598	-0.0113	-0.1031	-0.1146	-0.705
Clp	<i>roll damping</i>	-0.45	-0.3579	-0.3702	-0.3630	-0.3630	-1.2217	-3.2200	-4.0508	-11.39962
Clr	<i>roll due to yaw</i>	0.265	0.0755	0.1119	0.0839	0.0886	0.0150	0.2922	0.3495	3.26038
CIDa	<i>roll control power</i>	0.161	0.2652	0.1810	0.2650	0.2650	0.3436	0.1373	0.4509	2.5377
CIDr	<i>roll due to rudder</i>	-0.00229	0.0028	0.0036	0.0027	0.0064	0.0076	0.0582	0.0052	0.17639
Cm0	<i>pitch moment at $\alpha = 0$</i>	0.194	0.0364	0.051	0.0438	0.0080	0.0272	0.0344	0.0974	0.00052
Cma	<i>pitch moment due to angle of attack</i>	-2.12	-1.0636	-0.5565	-0.8360	-2.0510	-1.9554	-2.2918	-2.4694	-0.162
Cma_dot	<i>pitch moment due to angle of attack rate</i>	-11	-4.6790	-3.7115	-2.0900	-5.2860	-5.2860	-1.9698	-2.0695	-3.6114
Cmq	<i>pitch moment due to pitch rate</i>	-36.6	-11.6918	-8.8818	-6.1300	-16.5200	-9.5805	-7.7120	-8.4569	-1.46052
CmDe	<i>pitch control power</i>	-1.76	-1.2242	-1.0469	-0.8490	-2.0210	-2.4808	-1.0422	-1.0273	0.19587
Cnb	<i>weathercock stability</i>	0.109	0.0484	0.0575	0.0278	0.0562	0.0804	0.0573	0.0573	1.11
Cnp	<i>adverse yaw</i>	-0.11	-0.0358	-0.0537	-0.0407	-0.0407	-0.0557	-0.2063	-0.2693	-0.71648
Cnr	<i>yaw damping</i>	-0.2	-0.0526	-0.0669	-0.0232	-0.0439	-0.1422	-0.3323	-0.3782	-4.10148
CnDa	<i>aileron adverse yaw</i>	-0.02	-0.0258	-0.0272	-0.0294	-0.0296	-0.0165	0.0004	-0.0045	0.17158
CnDr	<i>yaw control power</i>	-0.0917	-0.0326	-0.0388	-0.0186	-0.0377	-0.0598	-0.0052	-0.0586	-0.64458

Table 2. Geometry and mass/inertia data for different aircraft

		Pioneer	Bluebird	FROG	Silver Fox	Rascal	P10B	Pitbull
S	<i>reference area of wing, m²</i>	2.826	2.0790	1.6260	0.6360	0.4595	4.9161	8.94
b	<i>wingspan, m</i>	5.151	3.7856	3.2250	2.4100	2.8042	6.4516	8.13
c	<i>mean aerodynamic chord, m</i>	0.549	0.549	0.500	0.264	0.164	0.762	1.1
m	<i>gross weight, kg</i>	19	26.2	30.7	10.0	5.9	63.0	726
F	<i>fuselage length, m</i>		2.9	1.9	1.47	1.6535	3.2258	6.12
Ixx	<i>roll inertia, kgm²</i>		17.1	17.0	1.00	0.80	45.00	825
Iyy	<i>pitch inertia, kgm²</i>		17.9	11.4	0.87	0.70	29.00	1200
Izz	<i>yaw inertia, kgm²</i>		27.1	25.2	1.40	1.20	68.00	1240
CG	<i>% MAC on a thrust line</i>	33	27	34.5	25	25	25	25
V	<i>cruise velocity, m/s</i>	34	27	27	26	20	25	80
alphan rim	<i>trim angle of attack, deg</i>	6	3.8	5.25	3			

The moments of inertia (MOI) shown in this table for a prototype-deploying platform were obtained via the following rough formulas:

$$I_{xx} = I_{xx}^{ref} \frac{m}{m_{ref}} \frac{b^2}{b_{ref}^2}, I_{yy} = I_{yy}^{ref} \frac{m}{m_{ref}} \frac{F^2}{F_{ref}^2}, I_{zz} = I_{zz}^{ref} \frac{m}{m_{ref}} \frac{b^2}{b_{ref}^2} \quad (1)$$

The MATLAB code for MOI

```
Ixx=Data(6,2:6).*Data(4,7)./Data(4,2:6).*Data(2,7).^2./Data(2,2:6).^2
Iyy=Data(7,2:6).*Data(4,7)./Data(4,2:6).*Data(5,7).^2./Data(5,2:6).^2
Izz=Data(8,2:6).*Data(4,7)./Data(4,2:6).*Data(2,7).^2./Data(2,2:6).^2
```

where the matrix Data contains the data of Table 2, produces the following results:

```
Ixx =    2185    2555    826    827    823
Iyy =    2209    2797    1095    1180    1203
```

```

Izz = 3464 3787 1157 1241 1244

clc;
T=0.05;
r_lim=7;
% Initial Conditions in ENU (all vector data is represented as a column vectors)
Pos_0 = [0; 0; 300]'; % Initial position vector (m)
Euler_0 = [0; 0; 0]*pi/180; % Initial Euler angles (rad)
Omega_0 = [0; 0; 0]'; % Initial Omega (rad/s)
PQR_0 = [0; 0; 0]'; % Initial Omega (rad/s)
Vb_0 = [30; 0; 0]'; % Initial velocity vector in {b}(m/s)

% Mass and Geometric Parameters recomputation
S = 8.875737087; % surface area of wing (m2)
span = 8.126476; % wingspan (m)
chord = S/span; % chord (m)
mass = 726; % gross weight (kg)
Ixx = 825; % main moment of inertia around axis Ox (kg*sq.m)
Iyy = 1200; % main moment of inertia around axis Oy (kg*sq.m)
Izz = 1240; % main moment of inertia around axis Oz (kg*sq.m)

% Aerodynamic Derivatives (all per radian)
CL0 = -.00089; % lift coefficient;
CLa = 4.47; % lift curve slope
CLa_dot = 2.19; % lift due to angle of attack rate
CLq = 0.76614; % lift due to pitch rate
CLDe = 0.4888; % lift due to elevator
CD0 = 0.015; % drag coefficient at a = 0
Apolar = 0.081; % drag curve slope (A2)
A1 = 0.00025;
CYb = -0.709; % side force due to sideslip

```

```

CYDr  = 0.2063;    % sideforce due to rudder
Clb   = -0.705;    % dihedral effect
Clp   = -11.3996;   % roll damping
Clr   = 3.26038;    % roll due to yaw rate
ClDa  = 2.5377;     % roll control power
ClDr  = 0.17638;    % roll due to rudder
Cm0   = 0.00052;    % pitch moment at a = 0 =>0.0652
Cma   = -0.0162;    % pitch moment due to angle of attack
Cma_dot = -3.6114;  % pitch moment due to angle of attack rate
Cmq   = -1.46052;   % pitch moment due to pitch rate
CmDe  = 0.1958;     % pitch control power
Cnb   = 1.11;       % weathercock stability = 0.075
Cnp   = -0.71648;   % adverse yaw
Cnr   = -4.10148;   % yaw damping
CnDa  = 0.17158;    % aileron adverse yaw
CnDr  = -0.64458;   % yaw control power
CLDf  = 0;
CmDf  = 0;
% Standard Atmosphere
ISA_lapse = .0065;   % Lapse rate      (degC/m)
ISA_hmax  = 2000;    % Altitude limit  (m)
ISA_R     = 287;     % Gas Constant   (degK*m*m/s/s)
ISA_g     = 9.815;   % Gravity      (m/s/s)
ISA_rho0  = 1.225;   % Density at sea level (kg/m/m/m)
ISA_P0    = 101325;  % Sea-level Pressure (N/m/m)
ISA_T0    = 289;     % Sea-level Temperature (degK)

%%%%%%%%%%
%%%%%
% Load Wind Profile

```

```

%%%%%%%%%%%%%%%%%%%%%%%%%%%%%%%%%%%%%%%%%%%%%%%%%%%%%%%%%%%%%%%%%%%%%%%%
%%%%%%%%
load YPGwind.mat;
load track.mat;

%% Determine steady-state trim parameters
clc, V=norm(Vb_0); df=0;
ro=1.225*(1-0.0065*Pos_0(3)/288.15)^4.25589;
atrim = (CmDe*CL0*S*V^2*ro+CmDe*CLDf*df*S*V^2*ro-2*CmDe*mass*ISA_g-
CLDe*S*V^2*ro*Cm0-CLDe*S*V^2*ro*CmDf*df)/S/ro/V^2/(-
CLa*CmDe+Cma*CLDe);
detrim= -(Cma*CL0*S*V^2*ro+Cma*CLDf*df*S*V^2*ro-2*Cma*mass*ISA_g-
CLa*S*V^2*ro*Cm0-CLa*S*V^2*ro*CmDf*df)/S/ro/V^2/(-CLa*CmDe+Cma*CLDe);
% Cmtrim=Cm0+CmDf*df+Cma*atrim+CmDe*detrim
% CLtrim=CL0+CLDf*df+CLa*atrim+CLDe*detrim
atrim=atrim*180/pi
detrim=detrim*180/pi
CLtrim=mass*ISA_g/(S*ro*V^2/2);
Thrusttrim=(CD0+A1*CLtrim+Apolar*CLtrim^2)*S*ro*V^2/2
%% Introduce initial guesses on varied parameter(s)
%x0=[.15; -2]; % Guesses on throttle setting and detrim
x0=[Thrusttrim/244.5]
delev=detrim;
global delev throttle
%% Run optimization routine
options=optimset('TolFun', 1e-2, 'TolX', 1e-2, 'Display', 'iter');
[x,fval]=fminsearch(@DMfun, x0)
function f = DMfun(x0)
global delev throttle
throttle=x0(1);

```

```
%delev=x0(1);  
opt = simset('SrcWorkspace', 'base');  
sim('UAVtrim', [0 30], opt);  
f=yout(length(yout));
```

C. MODELING

Using the aerodynamic and control derivatives from previous sessions, we were able to develop a dynamic model in the Simulink environment in order to evaluate the quality of its flight characteristics.

With this model, we are able to find trimming conditions, computation of aerodynamic forces and moments of inertia. Taking into consideration the aerodynamic coefficients, we can determine the overall controllability and performance of the model.

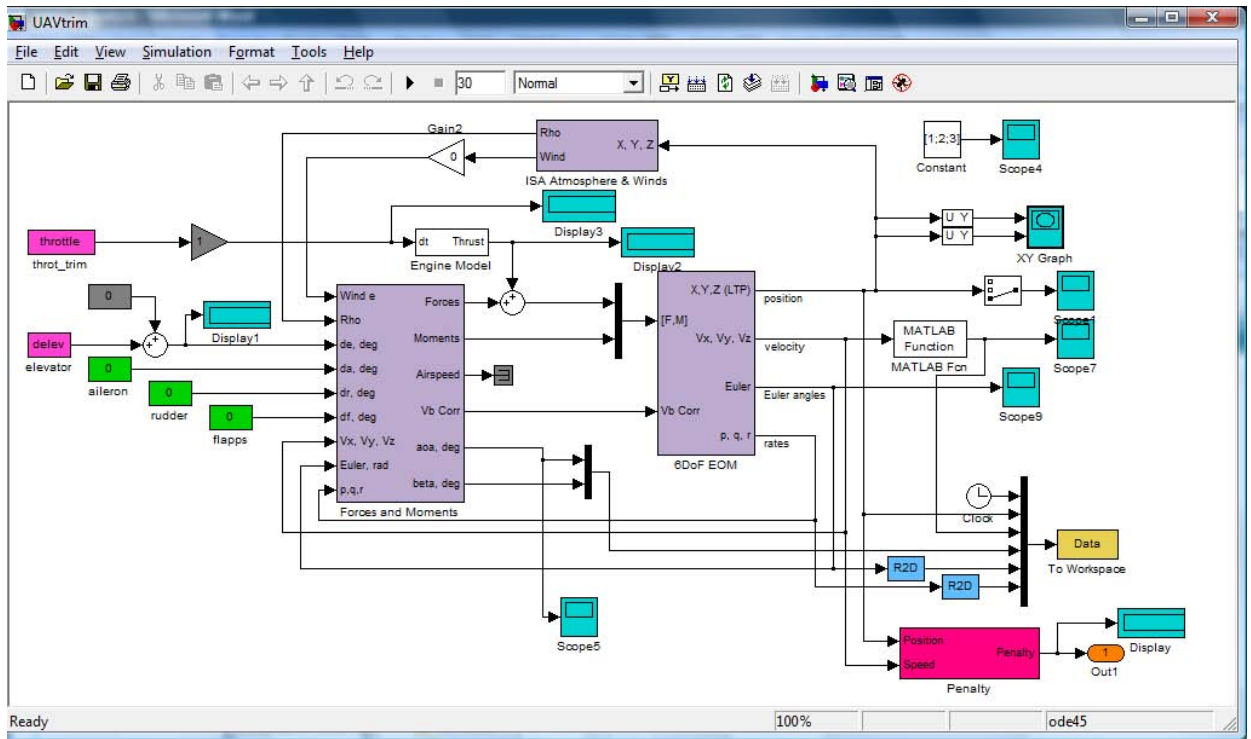


Figure 17. Simulink model for finding trim conditions

The first step was to determine whether the UAV is stable under trim condition. As we can see in Figure 17, the short-period motion dies fast, in fractions of a second. It is continuous by a long-period motion of small amplitude.

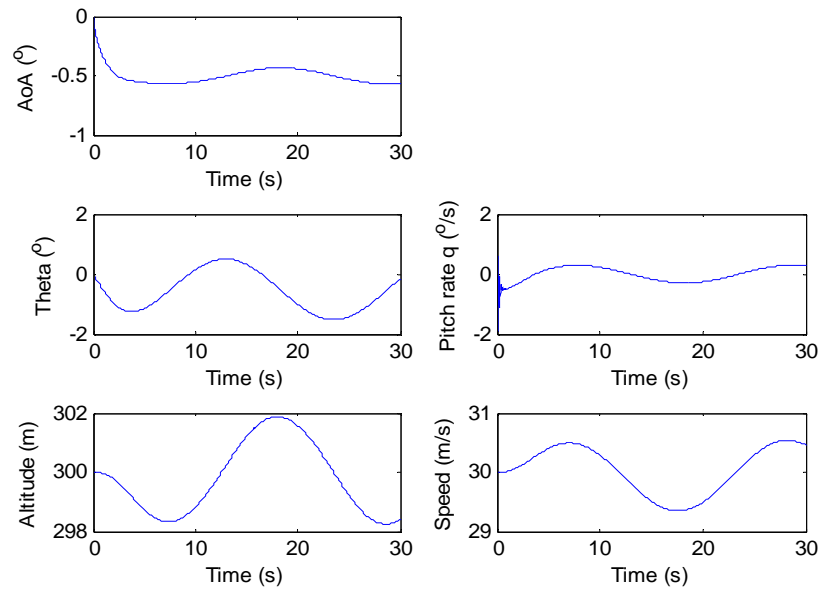


Figure 18. Pitbull longitudinal channel at trim condition

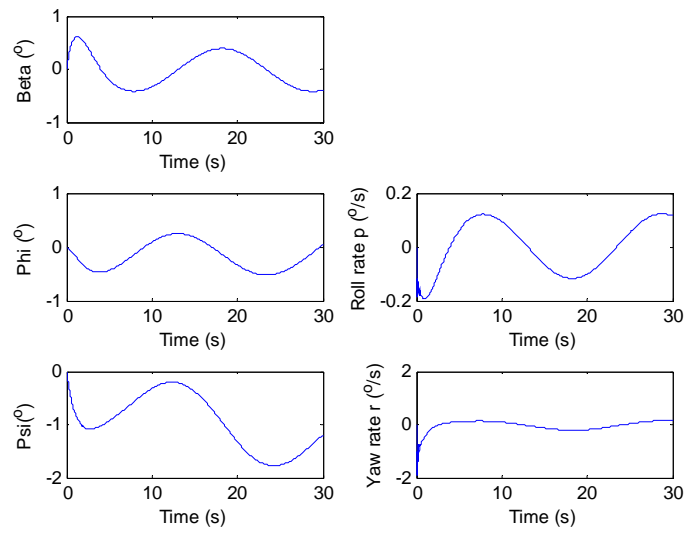


Figure 19. Pitbull lateral channel at trim condition

Once the trim condition of the UAV was verified, a series of tests were done to verify the dynamic response. For example, Figure 20 presents a response to the step increase of the thrust (by 10%)—the aircraft starts climbing. Figure 21 shows the response to a -1° elevator deflection.

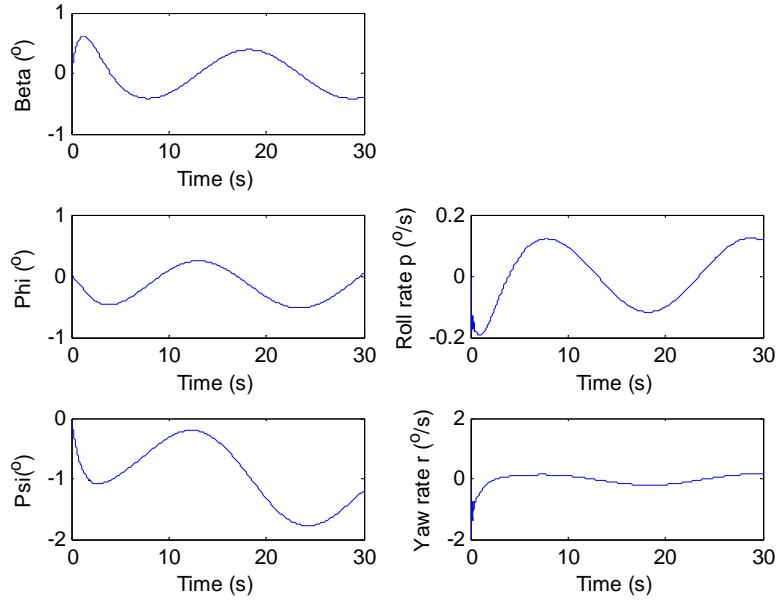


Figure 20. Pitbull longitudinal channel with 10N throttle increase

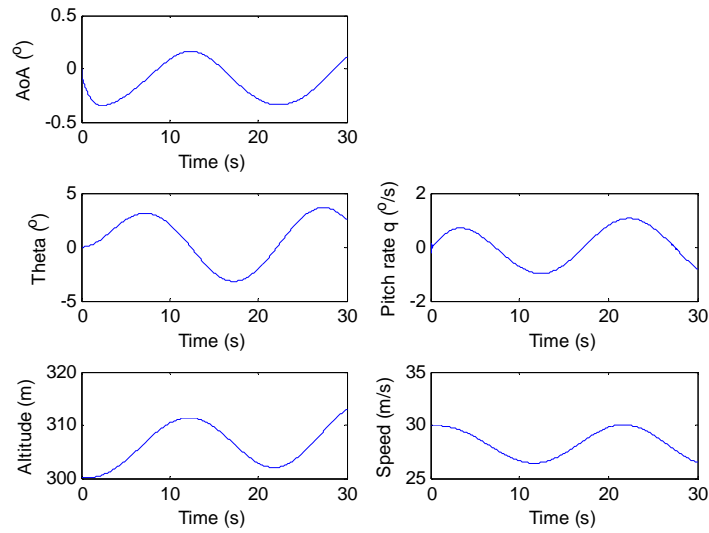


Figure 21. Pitbull longitudinal channel with 1 degree elevator deflection

Other tests were conducted for the lateral channel. Finally, Figure 22 shows the UAV rolling as a response to a -1° aileron deflection, and Figure 23 shows the response to -1° rudder deflection.

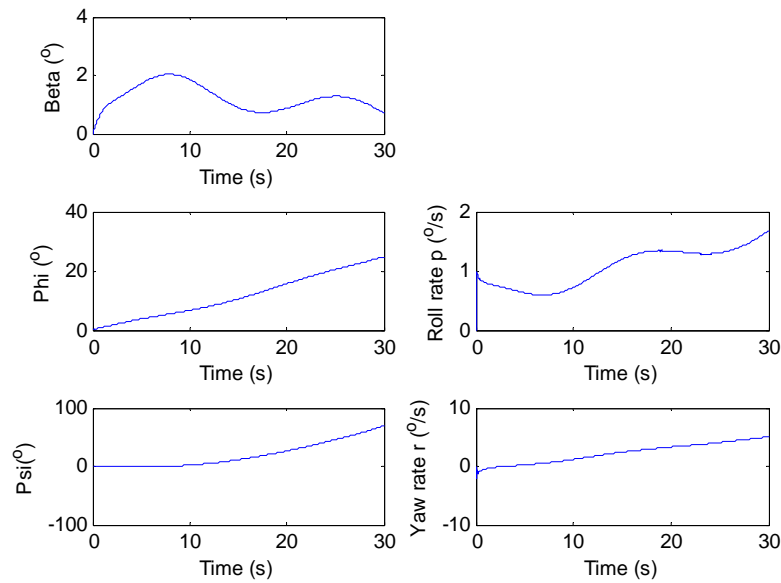


Figure 22. Pitbull lateral channel with 1 degree aileron deflection

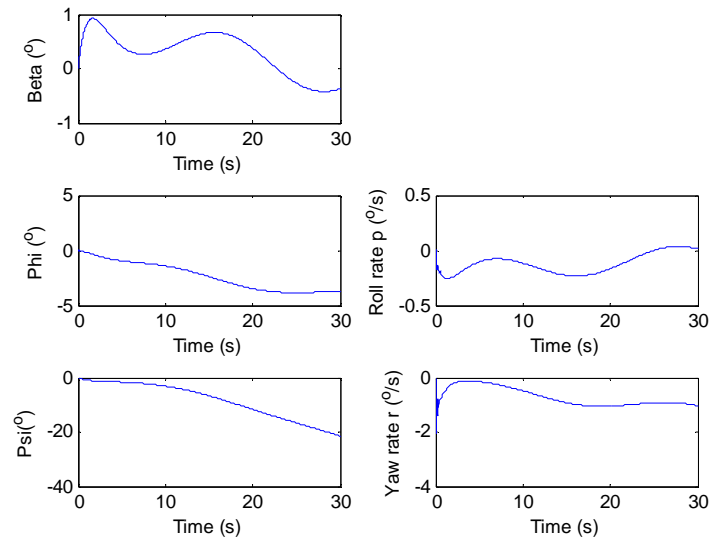


Figure 23. Pitbull lateral channel with 1 degree rudder deflection

By design, GSM is a cellular network, and coverage can be established through several cells. The result is that every mobile phone is connected with the nearest cell. According to size, the cells are called macro, micro, pico, femto or umbrella. Macro is the most basic cell, generally installed in the highest buildings. In contrast, micro cells are used in urban areas, as the height of their installation is below the average height of the surrounding buildings. Pico and femto are smaller cells, designed to be used indoors or in small industries. Finally, umbrella cells, are used to fill the gaps between the smaller cells. The coverage distances depend on the antenna's characteristics concerning aperture, gain, propagation and position. The GSM distance limit is 22 miles [4].

GSM operates on a variety of frequencies. The 2G (second generation) network operates at 900MHz or 1800Mhz (U.S.) and the 3G (third generation) at 2100Mhz (Europe). The uplinks use frequencies from 890 to 915Mhz (from mobile to station) and the downlinks from 935-960Mhz (station-mobile) through 124 RF channels spaced at 200Khz.

The GSM network, in order to provide services like voice calls and SMS, is divided into other subsystems: the BSS (Base Station Subsystem) the NSS (Network and Switching Subsystem) and the GPRS Core Network.

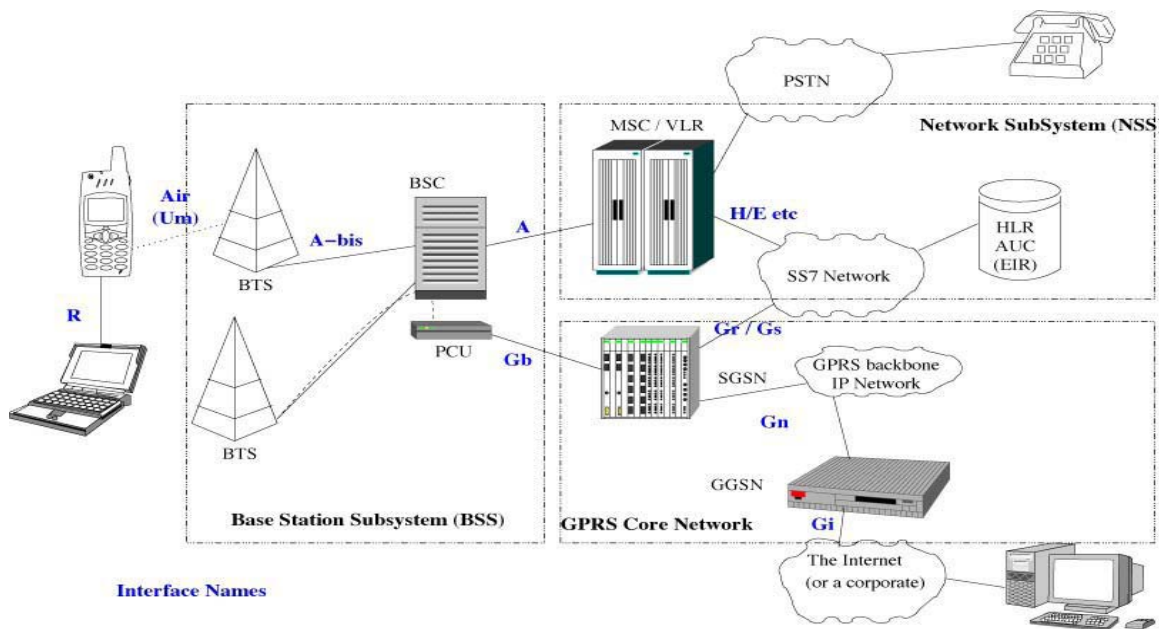


Figure 25. The structure of a GSM network

In Figure 25, we can see the three parts of a GSM network where the BSS includes the main controllers and stations connected with NSS, which is a classic design network. The GPRS part is optional and allows the GSM to be connected to the Internet.

This system is a powerful tool and consists of voice control. This is useful for operators who cannot handle the situation in front of a computer screen because of the overload. It is more feasible to control unmanned systems with voice communication, especially in a battlefield environment [5].

B. VOICE ON TARGET

Voice-based control formats and applications such as VoiceXML, for interactive communication between human and computer, are unique methods for controlling platforms, sensors, and UAVs via the GSM network. The ability that GPRS provides the ability for a network that can be connected to the Internet, which helps extend the distance of the communication between the operator and the platform worldwide. This means that the human can send and receive information from unmanned systems—from the screen of a laptop computer—and can also hear, speak, and give orders that generate immediate results.

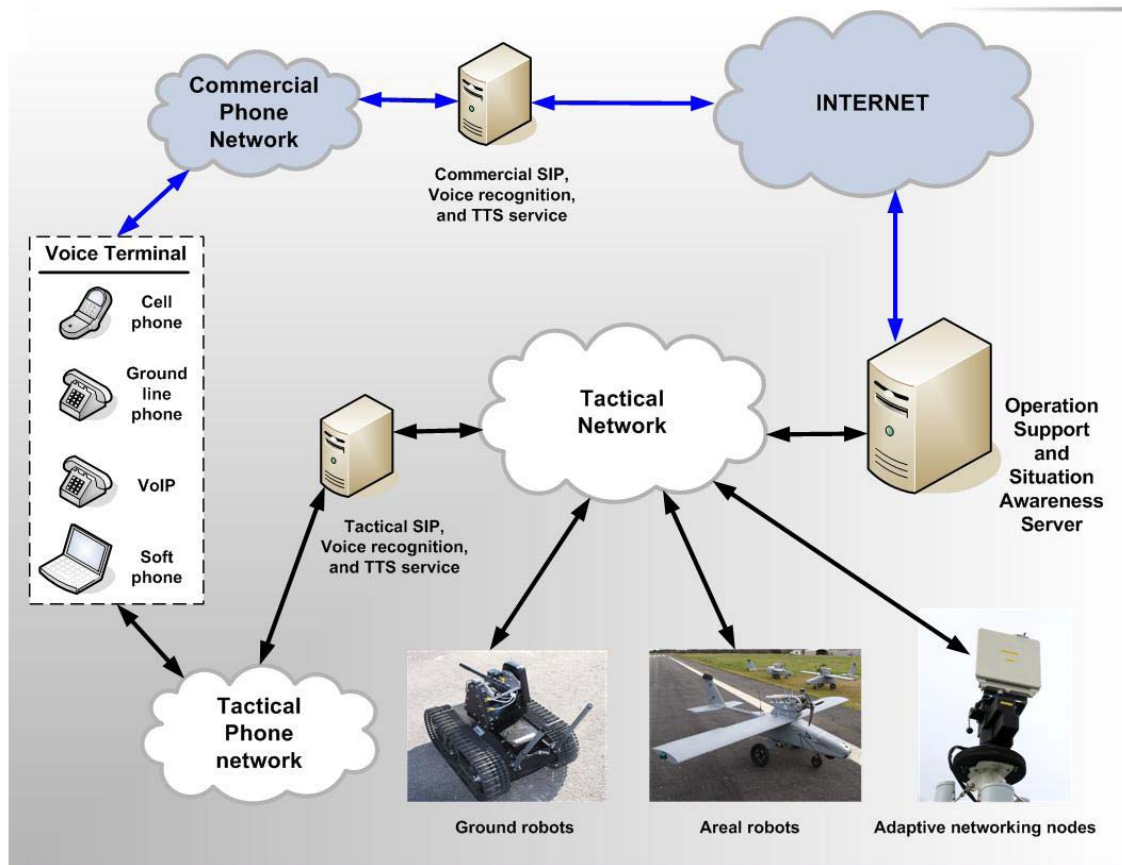


Figure 26. Voice-on-Target Portal Infrastructure

This method of communication—between humans and unmanned systems, sensors, and robots using “human language” and sharing the situation information—is called the Voice-on-Target approach. It provides platforms with the ability to “speak” back to their operators with a synthesized voice.

In Figure 26, we can see the general design of a Voice-on-Target Portal Infrastructure controlling robots and sensors. The voice commands can be transferred via Internet or via a tactical local area network and executed by the robots/sensors or unmanned vehicles. The benefit is that there is global coverage and that command and control can be conducted from a regular phone, a cell phone, VoIP or Soft Phone as a voice terminal device [6].

C. TNT TESTBED

A team of Naval Postgraduate School researchers, sponsored by the U.S. Special Operations Command (USSOCOM), Department of Homeland Security (DHS), and Office of the Secretary of Defense (OSD), developed an experimentation program, the Tactical Network Testbed (TNT) experiments. This testbed provides connectivity and integration between sensors, unmanned systems, networks and operators. The TNT users can connect their networking elements via an unclassified, closed IP space by getting fixed IPv6 addresses. They can also be connected with the testbed from local area networks via VPN (Virtual Private Network) or commercial IP cloud services. The VPN is also extended to a commercial satellite link into the Riverine operating area near San Francisco Bay. The VPN aims the users toward the public Internet and shares data with a secure system [6].

An important networking capability is one that enables plug and play, tactical-on-the-move sensors, unmanned systems, and situation awareness systems with global accessibility from the users by remote control. This means that operators can connect through a wide area network or other operational areas; in parallel, sensors and unmanned vehicles can be integrated with the TNT environment through the 802.16 link network.

The standard of this network defines the use of bandwidth from 10Ghz to 66Ghz (licensed) and from 2Ghz to 11 Ghz (licensed and unlicensed). The connection via 802.16 Wireless Communication Standard provides reliability, a higher throughput range, and greater distance coverage than 802.11.

The TNT interagency experimentation program is divided into two big fields. The first field involves NPS students and researchers from other universities with collaboration with USSOCOM, other government organizations, and any other participant that is involved with sensors, tactical networking, unmanned systems, situation awareness systems, biometrics, tactical decision makers, and managers focusing on high value target (HVT) tracking and surveillance missions [7].

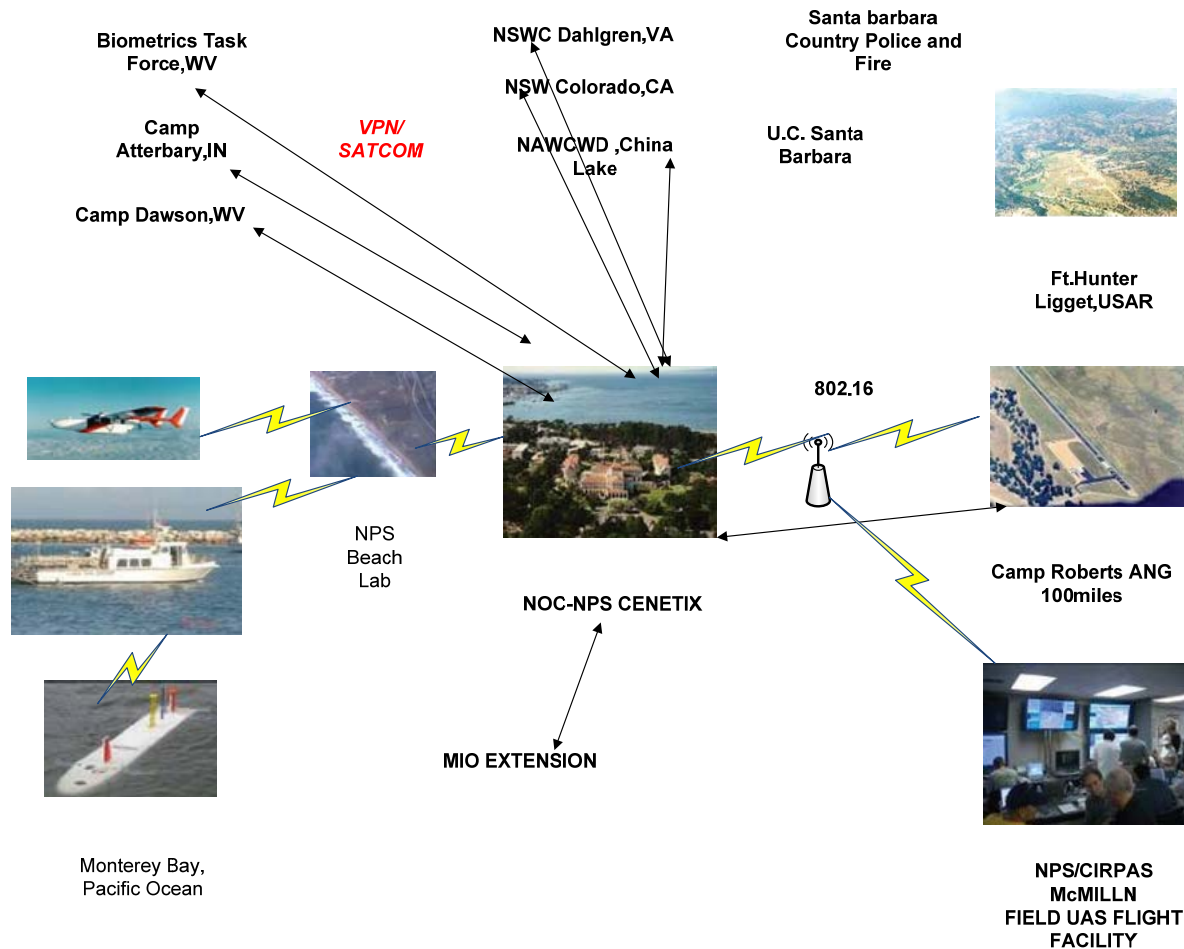


Figure 27. Plug-and-Play testbed with global reachback [7]

The second field of experiments is Maritime Interdiction Operation (MIO), supported by Homeland Defense (HLD) and HLS S&T Programs and the Department of Energy (DoE) agencies. This part of the TNT testbed is collaborated with Lawrence Livermore National Laboratory, USCG and First Responders (San Francisco Bay, New York/New Jersey), and is conducted twice a year in many places overseas. The experiments focus on searching large cargo vessels and interdicting small craft possessing nuclear radiation threats [7].

V. PITBULL-SNOWFLAKE COLLABORATION

Traditionally, UAV systems' applications and missions were communication relays for Intelligence Surveillance and Reconnaissance. Today, UAV systems, due to their importance and their ability to carry payloads and sensors, can be used in the battlefield for high-risk missions

A. SNOWFLAKE

One interesting payload, called Snowflake, is a miniature ADS (Aerial Delivery System), which the U.S. Special Operations Command sponsored as a project. It provides precision airdrops with high touchdown accuracy in order to minimize the risk to personnel, and with low cost. Snowflake is an autonomous payload that can be carried from a UAV. It can be used for delivering medicines, sensors, robots, supplies or any other material for the troops. The payload is attached to a rectangular parachute called a parafoil, which allows Snowflake to steer in the direction needed and proceed with high accuracy toward the target. The steering of the parafoil is controlled by actuators powered by electric motors [8].



Figure 28. Snowflake with parafoil (a) and avionics (b)

The fully deployed parafoil system is shown in Figure 28. We can see the payload container, which is a Pelican 1200 case that includes the guidance, navigation and control unit (GNC). It also contains accelerometers, a manometer, gyroscopes, a global position system (GPS) receiver, a barometric altimeter and an autopilot processor. The main idea is to move two servo motors for the control lines and to give guidance to the parafoil system.

The Snowflake weighs 4.3 lbs and is powered by standard rechargeable 7.4V 2100mAh batteries; its dimensions are 10.62'' x 9.68'' x 4.87''. The “free” space of the interior is about 83 percent of the total, so it can carry about 4 to 5 pounds of payload [9].

Other qualities of the system include a descent rate of 12 ft/sec, a glide ratio of 2, a forward speed of 14 knots, and a turning radius of 500 feet. The original system was developed to be deployed manually from a person inside an aircraft or helicopter. The Snowflake steers autonomously to the target with a CEP of 35 meters [10].

Many Snowflakes descending in different areas can establish a large distribution, as far as time and space and network, by carrying sensors that communicate with each other. Furthermore, their remotely controlled parafoils make it possible for individual nodes or hubs for a short-term aerial-to-ground network. This can be accomplished by placing a small base in the payload and allowing it to have a gradually descending wireless network, and sharing information with another group of Snowflakes via UAV or a ground station.

B. PITBULL AS A CARRIER OF SNOWFLAKES

The last edition of the previous system is Snowflake–N (Networked Snowflake). This prototype includes a Blackberry 8310 cell phone connected with the autopilot via Parani-ESD200 Bluetooth and allows communication with other network clients via GSM. Its most important capability is that an operator can communicate with the Snowflakes, not only via GSM (voice or SMS), but also via the Internet, and pass new information about the targets or change the mission profile. In addition, a system of Snowflakes can be used as the innovative node of an ad-hoc self-forming network because of the system’s ability to share information [8].

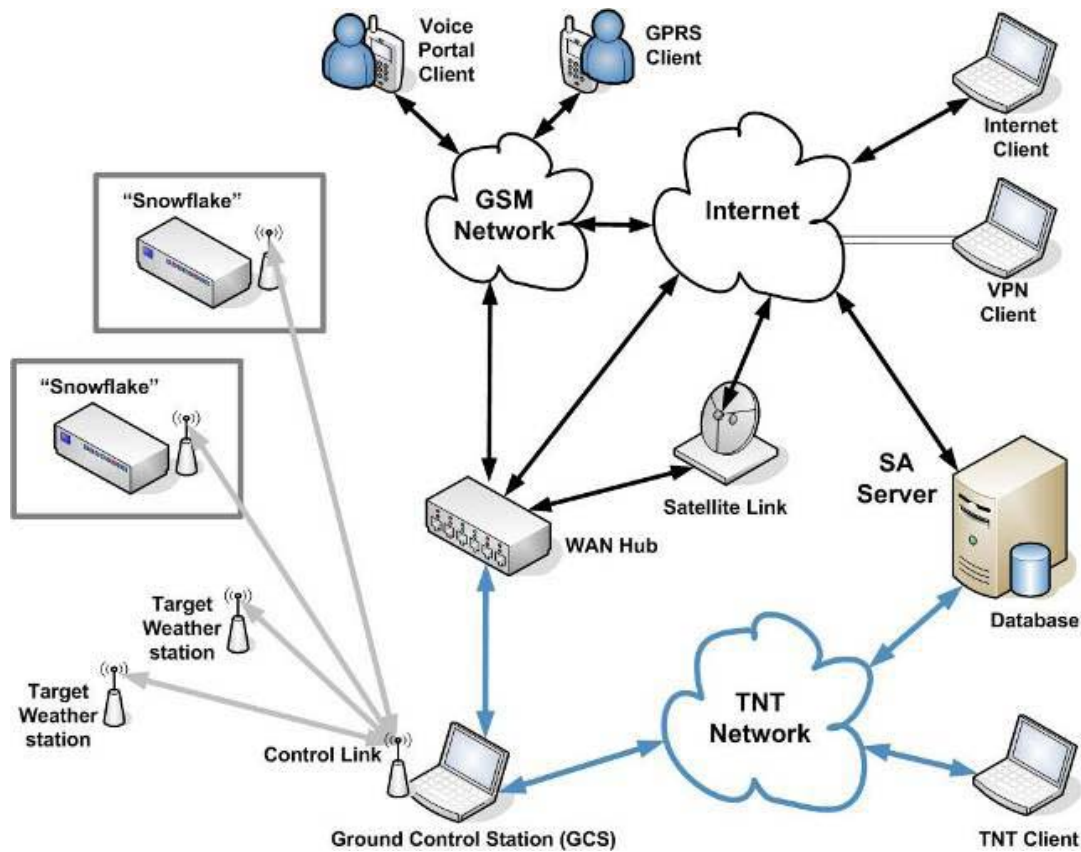


Figure 29. The Snowflake communication architecture [8]

Furthermore, the system can also be connected with TNT, and allow a bidirectional communication for sending and receiving new information through multiple sensors or users/operators from anywhere in the world, back and forth to the descending Snowflakes. When necessary, they can update their data and change the profile of the mission [8].

A large UAV such as Pitbull can carry about a dozen Snowflakes. Taking into consideration that this future UAV concept will be controlled the same way as the Snowflakes, we can anticipate a powerful tool for difficult missions.

Controlling the UAV from a GSM network or via link 802.16, or connected to a Network Operational Center (NOC) through TNT testbed, creates the opportunity to change the mission parameters every moment. This means that the UAV can distribute Snowflakes in areas where the information is constantly changing, such as a search and

rescue, which is a dynamic and complex operational scenario. Different capabilities are required for successful operations, such as monitoring points of interest that are not well known. In emergencies, such as earthquakes or tsunamis, it would be very useful if an injured person could send a SMS with his geo-coordination via GSM to a control center.

At that point, the operator could upload or send the data to the autopilot of the UAV and steer it to a specific area. Snowflakes can carry relief packages of medicines, food or other supplies; cameras onboard can send photos back to the control center to evaluate the importance of the situation.

Another option for using the complete system is the Pitbull-Snowflake, which can improve the accuracy of the descending Snowflake. While dropping a Snowflake from a height until it touches the ground, its autopilot must constantly make “corrections” to drive the parafoil to the correct the path and compensate for the wind. The most important factor is that the wind is changing continuously during the descent, so the autopilot has to make many corrections for the optimum flight path. The original concept was that the descending Snowflake was to receive weather data from ground sensors. The problem was that when the autopilot received the new wind data and made its path corrections, it took a little too long because of the slow reaction of the parafoil-canopy. Thus, by the time the steering correction was made, new data indicated that the wind had already changed [9].

A good solution for this problem could be to drop the Snowflake from the UAV with free diving, after taking into consideration ballistic tables for finding the release point. Also, the autopilot could be reprogrammed to open the canopy at the minimum height that is optimum, to slow the Snowflake prior to landing with a safe speed. This would cause fewer corrections for the parafoil and would increase the accuracy, especially if the near-landing winds are known by the weather sensors. The last scenario is feasible only in friendly areas because we must get information from weather sensors. In addition, the UAVs have to travel close to the target because of the short release range, and this can be extremely dangerous for missions in the battlefield.

In addition, the Snowflakes' abilities to communicate with each other and the UAV can be useful for increasing their accuracy. This scenario can be applied in every mission that needs precision and reliability. After choosing the target and designing the profile of the mission, we can let the Pitbull travel to the optimal point for a single drop and then move to a point where the link is strong enough for receiving data from the Snowflake. While descending to the target, the Pitbull can collect wind data every 1,000 feet and uplink them to the UAV and/or the rest of the Snowflakes. In this way, all the rest of the drops for this particular area will get a precise estimate for the winds at every level; this will dramatically increase the accuracy and the effectiveness of the mission.

The Pitbull-Snowflake system can be an important platform and can bring sensors or robotics for multiple missions, such as finding radiation or chemical environments, and pass the information directly to the Pitbull, which can then be used as a relay between the Snowflakes and the control center. When several Snowflakes are deployed and are gradually descending, they can develop a short-term, aerial-ground, ad-hoc network because of their ability to communicate between each other as well as with the Pitbull-UAV. This ability can extend the distance between the Snowflakes and offers the opportunity to cover large areas with better reliability on communication and the transfer of data.

C. MULTIPLE SNOWFLAKES CREATING AN AD-HOC NETWORK

Nearby nodes can communicate directly by a single-hop wireless technology (e.g., Bluetooth, 802.11, etc.), while devices that are not directly connected communicate by forwarding their traffic via a sequence of intermediate devices. Generally, the users' devices are mobile, and these networks are often referred to as Mobile Ad hoc NETWORKs (MANETs) [11].

Mobile Ad Hoc networks are a connection between moving nodes via a wireless link. The nodes can be self-organized into arbitrary and temporary ad-hoc network topologies and give the opportunity to create a tactical network to areas without pre-existing communication facilities and specialized scenarios, such as disaster recovery, vehicle-to-vehicle communications, and hostile environments.

In ad hoc networks, nodes can transfer data to each other without a fixed infrastructure. Most of the time, these kinds of networks consist of hosts that communicate over wireless links without any central control.

The ad hoc wireless networking technology provides many advantages in the battlefield because they are self-organized and have flexibility and instant deployment. These kinds of networks inherit the traditional problems of wireless and mobile communications, such as bandwidth optimization, power control, and transmission quality [12].

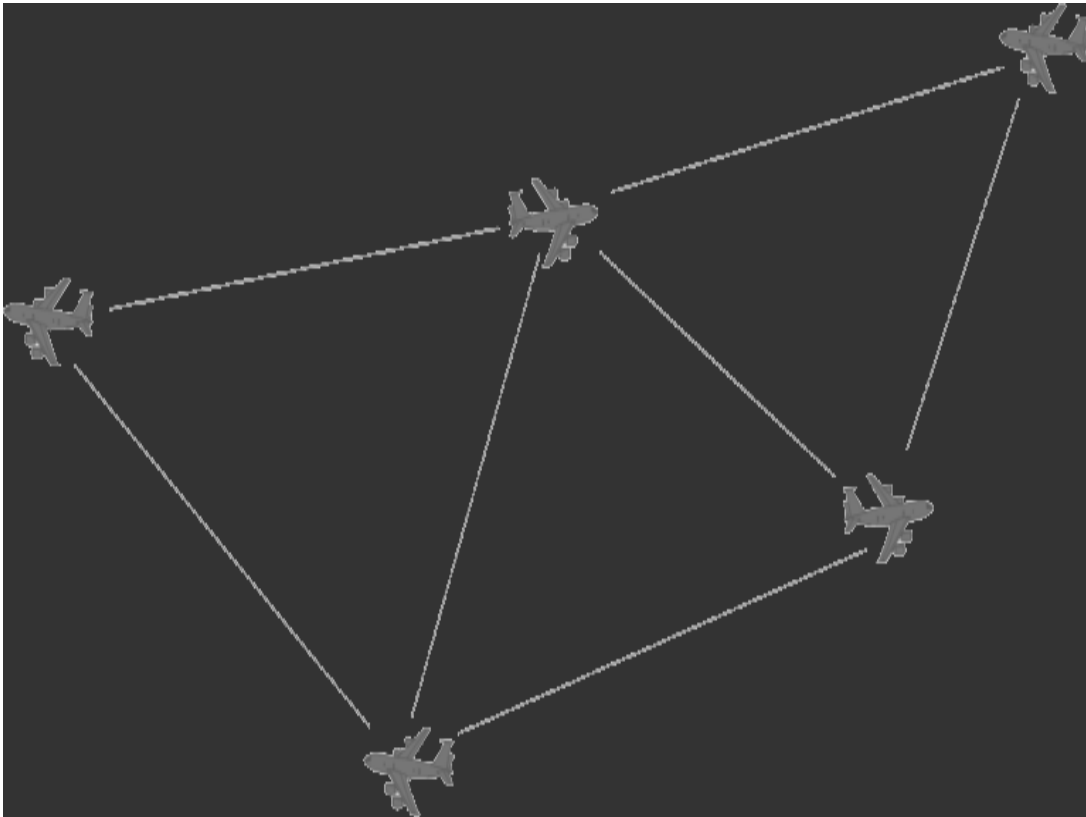


Figure 30. UAVs creating ad-hoc network

UAVs enroute can create an ad-hoc network for sharing information such as weather conditions and data sharing, and can avoid mid-air collisions, take orders from the mission controllers, and change their mission profile.

An interesting dynamic scenario can be an ad-hoc network consisting of UAVs carrying Snowflakes. Since groups of Snowflakes, carried by UAVs, will operate autonomous or remotely in a hostile environment, UAVs can fly as a group for their specific mission in the area of interest and deploy their Snowflakes. The result would be wide network coverage, something useful in large territories where the mission is to create a network umbrella with sensors.

Snowflakes are slow movers, so we can consider their network topology a stable one. On the other hand, they have been pre-programmed to follow a specific tack; thus, there are no rapid fluctuations or connection interruptions in their network topology.

Considering that the conditions in these dynamic scenarios are continuously changing, the Snowflakes/nodes must continuously keep their connection even with the UAV, or with each other, for updating data and avoiding mid-air collisions. The transmission range between the Snowflakes, however, will be limited to their battery power.

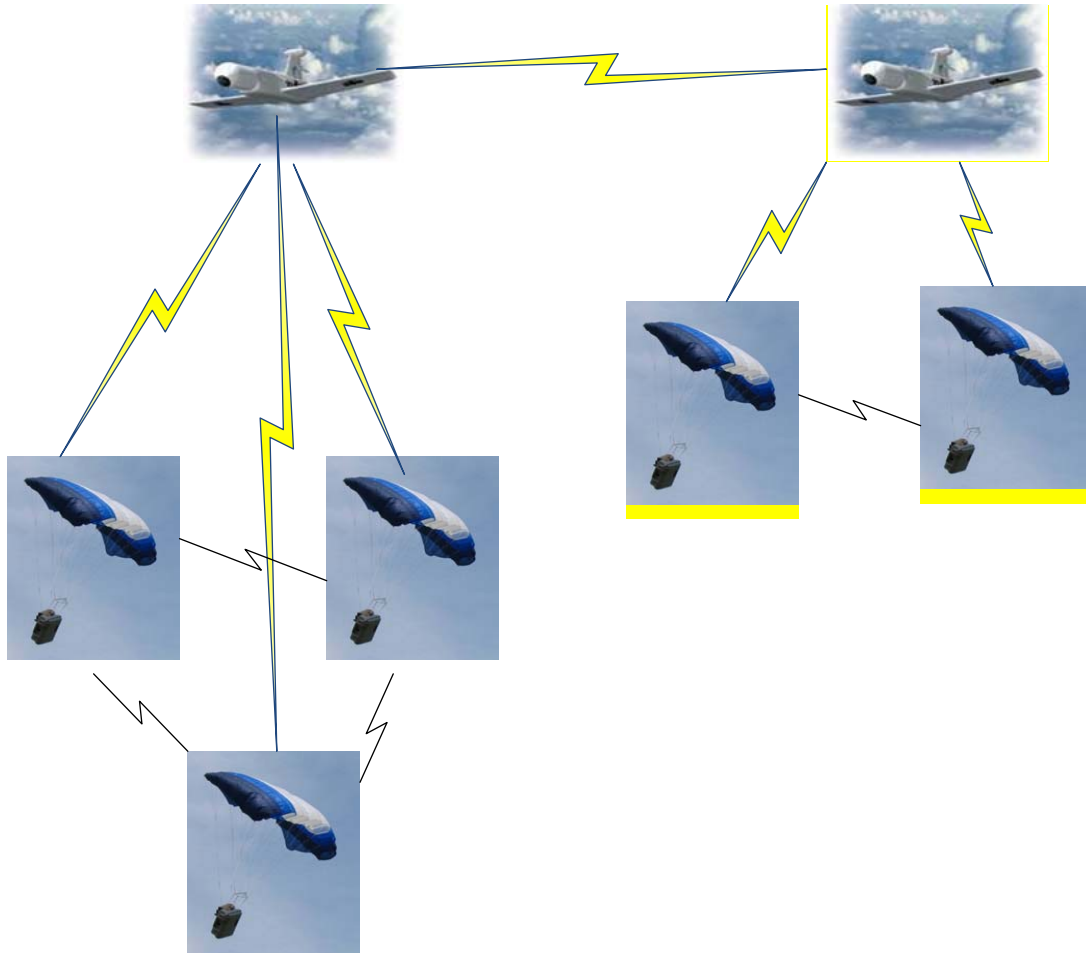


Figure 31. Group of UAVs carrying Snowflakes developing a short-term aerial ad-hoc network

Beyond the previous scenario, and adding this concept to the network system, UAV-Snowflake ad-hoc networks, GSM, Internet, and TNT testbeds, we get a large network concept that makes it possible to control multiple groups of UAVs carrying and dropping autonomous or remotely controlled Snowflakes with sensors.

VI. CONCLUSIONS

This thesis presents the development of a low-cost, large UAV as a platform to deploy multiple aerial delivery parafoil-based systems, such as Snowflakes, and to establish and exploit temporary on-the-go networks to relay data with the ability to be useful in other missions as well.

The Pitbull-Snowflakes system is expected to be a powerful tool for combat and peace, and should deliver a self-contained mobile system for precise aero delivery with a global-reach capability. Pitbull-UAV presents an ideal deployment platform and an alternative low-cost suggestion with the capability of carrying payloads, as well as co-operation with the Snowflake system. The design of multiple mobile Ad-hoc NETWORKS (MANETs) is not simple. Further research and development are needed to find the best routing network protocol because, as the size of a multi ad-hoc network grows, the performance tends to decrease [13].

The co-operation of the system UAV-Snowflake with the TNT testbed through GSM and the Internet can be an alternative approach for communication between man and the tactical network environment, and improve the method of transferring information and orders, sharing information, and getting real-time picture and situation awareness from the area of interest.

THIS PAGE INTENTIONALLY LEFT BLANK

LIST OF REFERENCES

- [1] “MQ-9 Reaper: The First Operational UCAV?” *Defense Industry Daily*, June 10, 2010.
- [2] “GSM World Statistics,” GSM Association, 2007.
- [3] “About GSM Association,” GSM Association, April 2009.
- [4] “Two Billion GSM Customers Worldwide,” 3G Americas, June 13, 2006.
- [5] E. A. Bourakov, O. A. Yakimenko, and N. J. Slegers, “Exploiting a GSM Network for Precise Payload Delivery.” Proceedings of the 20th AIAA Aerodynamic Decelerator Systems Technology Conference, Seattle, WA, May 4–7, 2009.
- [6] Dr. Alex Bordetsky and Dr. David Netzer, “Testbed for Tactical Networking and Collaboration,” *The International C2 Journal* 4, no.3, 2010.
- [7] Dr. Alex Bordetsky and Dr. David Netzer, “TNT Testbed for Self-Organizing Tactical Networking and Collaboration,” Proceedings of the 11th International Command and Control Research & Technology Symposium, Washington, D.C, June 2009.
- [8] O. Yakimenko, N. Slegers, E. Bourakov, C. Hewgley, A. Bordetsky, R. Jensen, A. Robinson, J. Malone, and P. Heidt, “Mobile System for Precise Aero Delivery with Global Reach Network Capability.” Proceedings of the 7th IEEE International Conference on Control & Automation, Christchurch, New Zealand, December 9–11, 2009.
- [9] O. Yakimenko and N. Slegers, “Using Direct Methods for Terminal Guidance of Autonomous Aerial Delivery Systems.” Proceedings of the European Control Conference, Budapest, Hungary, August 23–26, 2009.
- [10] N. Slegers and O. Yakimenko, “Optimal Control for Terminal Guidance of Autonomous Parafoils.” Proceedings of the 20th AIAA Aerodynamic Decelerator Systems Technology Conference, Seattle, WA, May 4–7, 2009.
- [11] S. Basagni et al., eds., *Mobile Ad Hoc Networking*, IEEE Press, 2003.
- [12] Ivan Stojmenovic, Jie Wu, “Ad Hoc Networks,” IEEE Computer Society, February 2004.
- [13] Jon Crowcroft and Andrea Passarella (Univ. of Cambridge), *Multi-hop Ad hoc Networks from Theory to Reality*, Marco Conti (Inst. for Informatics and Telematics, Pisa, Italy).

THIS PAGE INTENTIONALLY LEFT BLANK

INITIAL DISTRIBUTION LIST

1. Defense Technical Information Center
Ft. Belvoir, Virginia
2. Dudley Knox Library
Naval Postgraduate School
Monterey, California
3. Chairman
Department of Information Science
Naval Postgraduate School
Monterey, California
4. Prof. O. Yakimenko
Department of Mechanical & Aerospace Engineering
Naval Postgraduate School
Monterey, California
5. Prof. A. Bordetsky
Department of Information Science
Naval Postgraduate School
Monterey, California
6. Instr. P. Atshian
Department of Electrical & Computer Engineering
Naval Postgraduate School
Monterey, California
7. Embassy of Greece
Office of Air Attaché
Washington, District of Columbia
8. MAJ Andreas Archontakis
Hellenic Air Force Staff
Athens Greece